Design of CTD Observational Programmes in Relation to Sensor Time Constants and Sampling Frequencies

R.G. Perkin and E.L. Lewis

Institute of Ocean Sciences
Department of Fisheries and Oceans
Sidney, B.C. V8L 4B2

1982

Canadian Technical Report of Hydrography and Ocean Sciences No. 7

Canadian Technical Report of Hydrography and Ocean Sciences

These reports contain scientific and technical information of a type that represents a contribution to existing knowledge but which is not normally found in the primary literature. The subject matter is generally related to programs and interests of the Ocean Science and Surveys (OSS) sector of the Department of Fisheries and Oceans.

Technical Reports may be cited as full publications. The correct citation appears above the abstract of each report. Each report will be abstracted in Aquatic Sciences and Fisheries Abstracts. Reports are also listed in the Department's annual index to scientific and technical publications.

Technical Reports are produced regionally but are numbered and indexed nationally. Requests for individual reports will be fulfilled by the issuing establishment listed on the front cover and title page. Out of stock reports will be supplied for a fee by commercial agents.

Regional and headquarters establishments of Ocean Science and Surveys ceased publication of their various report series as of December 1981. A complete listing of these publications and the last number issued under each title are published in the *Canadian Journal of Fisheries and Aquatic Sciences*, Volume 38: Index to Publications 1981. The current series began with Report Number 1 in January 1982.

Rapport technique canadien sur l'hydrographie et les sciences océaniques

Ces rapports contiennent des renseignements scientifiques et techniques qui constituent une contribution aux connaissances actuelles mais que l'on ne trouve pas normalement dans les revues scientifiques. Le sujet est généralement rattaché aux programmes et intérêts du service des Sciences et Levés océaniques (SLO) du ministère des Pêches et des Océans.

Les rapports techniques peuvent être considérés comme des publications à part entière. Le titre exact figure au-dessus du résumé du chaque rapport. Les résumés des rapports seront publiés dans la revue Résumés des sciences aquatiques et halieutiques et les titres figureront dans l'index annuel des publications scientifiques et techniques du Ministère.

Les rapports techniques sont produits à l'échelon régional mais sont numérotés et placés dans l'index à l'échelon national. Les demandes de rapports seront satisfaites par l'établissement auteur dont le nom figure sur la couverture et la page de titre. Les rapports épuisés seront fournis contre rétribution par des agents commerciaux.

Les établissements des Sciences et Levés océaniques dans les régions et à l'administration centrale ont cessé de publier leurs diverses séries de rapports depuis décembre 1981. Vous trouverez dans l'index des publications du volume 38 du *Journal canadien des sciences halieutiques et aquatiques*, la liste de ces publications ainsi que le dernier numéro paru dans chaque catégorie. La nouvelle série a commencé avec la publication du Rapport n° 1 en janvier 1982.

Canadian Technical Report of

Hydrography and Ocean Sciences No. 7

1982

DESIGN OF CTD OBSERVATIONAL PROGRAMMES IN RELATION TO SENSOR TIME CONSTANTS AND SAMPLING FREQUENCIES

by

R.G. Perkin and E.L. Lewis

Institute of Ocean Sciences

Department of Fisheries and Oceans

Sidney, B.C. V8L 4B2

Copyright Minister of Supply and Services Canada - 1982

Cat. No. FS 97-18/7 ISSN 0711-6764

Correct citation for this publication:

Perkin, R.G. and E.L. Lewis, 1982. Design of CTD observational programmes in relation to sensor time constants and sampling frequencies. Can. Tech. Rep. Hydrogr. Ocean Sci: No. 7:47p.

Table of Contents

	Page
Abstract	iv
Foreword	1
Summaries - How to design CTD observational programmes and compute data	2
- Advice to CTD manufacturers	4
Main text	
1. Introduction	5
2. Instrumentation	5
3. Sensor response	7
4. Sensor time constants and sampling considerations	10
5. Computer simulation of CTD observations	14
6. Application to field observations	26
7. Further data processing	31
Appendices	
I Sensor time constants and their adjustments	34
II Aliasing	39
III Running mean filters and block averaging	44
References	47

ABSTRACT

Perkin, R.G. and E.L. Lewis. 1982. Design of CTD Observational Programmes in Relation to Sensor Time Constants and Sampling Frequencies. Can. Tech. Rep. Hydrogr. Ocean Sci. No. 7:47p.

A discussion of sensor time constants and sampling frequencies leads to an exposition of problems and their solutions in computing parameters such as salinity, which are a combination of the outputs from two different sensors. A balance between the attenuation of useful inputs by sensor inertia, yet adequate rejection of energy aliased from higher frequencies, leads to optimum design criteria for CTD observational programmes. These criteria are explored by computer simulation and finally the principles are applied to produce useful improvements in field data. The discussion concludes by suggesting an appropriate procedure for elimination of "wild" values due to electronic malfunction or noise remaining due to the inability of the recommended procedures to correct for gross observational problems, such as those associated with violent changes in the CTD probe descent velocity.

RÉSUMÉ

Perkin, R.G. and E.L. Lewis. 1982. Design of CTD Observational Programmes in Relation to Sensor Time Constants and Sampling Frequencies. Can. Tech. Rep. Hydrogr. Ocean Sci. No. 7:47p.

Le présent rapport examine les constantes de durée de détection et les fréquences d'échantillonnage, ce qui mène à un exposé des problèmes et des solutions dans le calcul des paramètres (dont la salinité) qui résultent de la combinaison des données de deux capteurs. Un équilibre entre l'atténuation des entrées utiles, par suite de l'inertie des détecteurs, et un rejet suffisant de l'énergie empruntée de fréquences plus élevées mène à des critères optimums de conceptions des programmes d'observation CTP. Ces critères sont étudiés à l'aide d'une simulation sur ordinateur et les principles sont ensuite appliqués pour générer une amélioration utile des données recueillies sur le terrain. On conclut en suggérant une procedure appropriée pour éliminer des valeurs abracadabrantes causées par un mauvais fonctionnement électronique ou des résidue de bruit provoqués par l'inaptitude des procédures recommandées à corriger les gors problèmes d'observation, dont ceux associés avec des changements soudains de la vitesse de descente de la sonde CTP.

Foreword

This report has been written for technical as well as scientific staff concerned with the collection of oceanographic data. All significant mathematical manipulation has been relegated to the Appendices. Two "executive summary" type statements preface the report giving, without rationale, conclusions of potential use to those designing CTD observational programmes and instruments respectively.

The techniques advocated herein have enabled us to make major improvements to our data without resort to averaging or "despiking" procedures that are without a physical basis. Figure 12 may serve as an illustration of this. At this same time it is most important to realise that following our suggestions will not

(1) offer any improvement in signals contaminated by electrical noise arising in the CTD instrument itself or in the associated winch and deck equipment. Power supply stability, isolation from noise carried on the power lines, elimination of slip ring noise, etc. are as important as having stable electronics and sensors in the CTDs. A routine test for these faults should precede data collection. An outline of such a procedure is given in Lewis and Sudar (1972).

(2) offer any compensation for systematic errors resulting from poor sensor calibration or sensor instability. The stability of the conductivity sensor is, in our experience, the primary factor determining the limits of accuracy of CTD observations.

(3) be adequate in cases where the velocity of descent of the probe suffers major modulation due to ship movement. It is recommended that in extreme cases, where the velocity becomes negative during a cycle, the data should be discarded or used only to give an outline of gross features. Even with less violent movement the wake of the probe tends to "catch up" with and engulf it, making observations of fine structure impossible. As a general rule it is suggested that when the descent velocity minimum and maximum span a range greater than 1:2 extreme care should be used in interpretation of data. To start with, the results from the complete data set might be compared with sections of the same data selected as having been taken within small ranges of descent velocity. How do the signal fluctuations seen in data from a "slow" range of velocities compare to those seen in data from a "high" range, etc.?

A topic not explored herein, though frequently described in the literature, is that of an adjustment or deconvolution of data to regain the detail lost by the inability of sensors to respond fast enough to portray small scale oceanic features properly. If the data is good and the sensor characteristics are known, a "transfer function" may be designed for this purpose. However, the procedure is very susceptible to small errors in the data or just the general limits of accuracy of measurement and is falling out of favour. It is just too easy to produce large variations in the regenerated ocean from very minor changes in the input information. The procedure is not recommended.

The authors would be pleased to receive critical comment from those using this report.

HOW TO DESIGN CTD OBSERVATIONAL PROGRAMMES AND COMPUTE DATA

1. Decide the depth intervals for which representative salinity and temperature values are required, d. This means that the smallest wavelength required to be observed in the ocean is 2d.

2. Obtain the following measured values (may not be as quoted by supplier)
   (a) "Time constant"of the temperature sensor, τ_1. (time to 63% response)
   (b) "Time constant"of the conductivity sensor, τ_2.(time to 63% response)

   If this is not available consider 0.55 L/v as being equal to τ_2 where L is the length of the cell (or effective length for an inductive cell) along the direction of v, the probe descent velocity. If possible choose v so that $\tau_1 \sim \tau_2$.
   (c) Time interval δt between the measurement of conductivity and temperature values in a single sampling.
   (d) Time interval, Δt, between successive samplings of C, T and pressure.
   (e) Does the instrument record every sample (at intervals Δt) or does it record a block average of N samples (at intervals $N\Delta t$)?
   (f) Determine sensor separation, h (Figure 3).

3. If Δt is equal to or greater than τ, construct $\tau^* = \tau/\Delta t$ and $f^* = \Delta t v/d$ and enter Figures 17A and 17B to find the proportion of any energy available at wavelengths of less than $2\Delta t.v.$ which will be reflected into the desired part of the spectrum.

   This effect, called aliasing, is the appearance of spectral power from wavelengths causing sensor response, but too short to be detected by the sampling procedure, as an addition to power detected at the longer wavelengths. For example, spectral estimates given for a wavelength of 2d will be partially composed of spurious inputs from any power present at wavelengths of $2d/\left[2d/v\Delta t - 1\right]$, $2d/\left[2d/v\Delta t + 1\right]$ and other smaller wavelengths. Of course, these small wavelengths will tend to be attenuated by sensor inertia. This is why if Δt is smaller than τ, aliasing need not be considered at all.

4. Determine the power attenuation at the frequency of interest, v/2d, from the abscissa of Figure 17A and judge if it is acceptable/not acceptable.

5. If the values obtained from Figure 17A and 17B are judged as not acceptable, then alter "d" or the instrument time constants to suit, possibly by altering v for τ_2.

6. Proceed to make measurements, then calculate salinities by
   (a) applying a numerical filter as shown in Appendix 1 to slow down the response of the faster sensor (usually conductivity) to force τ_2 to equal τ_1. This filter is a function of the descent velocity v. If the data has been block averaged before recording over a time much longer than the sensor time constants ($N\Delta t \gg \tau_1, \tau_2$), this step can be omitted. It is usually necessary to smooth the pressure record in order to estimate the descent speed accurately.
   (b) If Δt (or $N\Delta t$) $\sim \tau$ interpolate one of the two time series for temperature and conductivity by $(\delta t - h/v)$ to compensate for the time between the reading of the two parameters (δt) and sensor separation (h). Alternatively, the sensor separation may be

adjusted so that $h = v\delta t$ and no interpolation is necessary. This physical separation is essential if Δt (or $N\Delta t$) is much greater than τ, making the interpolation inaccurate.

(c) Compute salinity from the filtered and interpolated time series.

7. Take average values over interval d from the time series for T and S after elimination of "wild" values due to electronic malfunctions by following Acheson (1975) or equivalent.

Example

Suppose it is required to resolve 0.5 m "slices" of an oceanographic profile (d = 0.5 m). τ_1 is given as 0.1s and L as 18 cm so that $\tau_2 = 0.55 \times 0.18/v$. If the sample interval Δt is 0.15s then $\tau^* = 2/3$ and from Figures 17A and 17B aliasing will be about 10%. If a record giving more than 80% of the power available at the desired 1 m wavelength is acceptable then from Figures 17A and 17B $f^* \leq 0.36$. Thus $v \leq 1.2$ m/s. To match time constants $\tau_1 = \tau_2$, $(0.55 \times 0.18)/v = 0.1$ giving $v = 1$ m/s. The physical separation between the sensors may now be adjusted to compensate for the time interval δt, between their sampling in a single record. If $\delta t = 0.05$s then $h = 1 \times 0.05 = 5$ cms. Alternatively and preferably, to cope with varying velocities of descent, (v variable) the time series for conductivity and temperature may be "slipped" i.e. interpolated by an interval $(h/v - \delta t)$ so that salinity calculation are carried out on values measured at the same location. Note that 7 measurements per metre have been necessary to resolve the desired half metre slice thickness adequately at the selected 1 m/s lowering speed. $f^* = 0.3$ and Figure 17 shows that the half meter signal is attenuated by only 15% by the sensor time constants, and that only 7% (Figure 17A) and 3% (Figure 17B) of any energy available at wavelengths of 18 cm and 13 cm respectively will appear aliased onto the 1 m wavelength record (d = 0.5 m).

Advice to CTD Manufacturers

1. Size your sensors so that the conductivity time constant (primarily descent speed dependent) equals the thermometer time constant, τ, (primarily thermal diffusivity dependent) at the average probe descent speed (about 1.0 m/s). If one of the sensors is significantly faster than the other, it will be necessary to "slow it down" in data processing in order to compute reliable salinity values.

2. Place the thermometer in a position with respect to the conductivity sensor so that both take their measurements at the same depth taking into account time delays within a single sampling sequence. In the case of a cell using electrodes, the response can be considered to be sensitive to water in the depth range covered by the cell only. Inductive cells, on the other hand, because of their less compact electrical field, must be considered to have a larger effective size. This size is best determined by experiment with any given inductive cell.

3. Design a sampling system so that at least one data point is collected per temperature time constant. This is particularly necessary when time constant compensation must be done in data processing as is frequently the case when lowering in a rough sea results in a varying conductivity time constant.

With this sampling rate, aliasing is effectively eliminated by the inertia of the sensors. However, much of the high frequency information is also attenuated so that only the lowest 10% of the discernable spectrum of oceanic variations is passed at greater than 90% of its power. Thus, the oceanic slice thickness which is accurately resolved by this system is $10v.\Delta t$ where v is the lowering speed and Δt is the sampling interval. If $\Delta t = \tau = 0.1$ s, $v = 1$ m/s, then salinity can be reliably calculated for every 1 m segment of the profile. In addition, finer scale features will be represented in attenuated form and can be enhanced by special filtering procedures though it is very difficult to place bounds on the quantitative validity of information so obtained. This performance is well suited to general oceanography.

1. Introduction

Conductivity-temperature-depth (CTD) probes of a variety of precisions are in common use and provide information of fundamental importance to oceanographers. Correct use of a probe can yield a wealth of information about the water and its dynamic state.

The most common form in which CTD data appears is as a profile obtained by lowering the instrument down through the water column while sampling the three variables, usually in a serial scheme. As the instrument moves through the water, it is desirable that the conductivity and temperature sensors be flushed as efficiently as possible so that values for these two variables may be properly assigned to the depth recorded at that time. The three variables may then be used in combination to produce profiles of the calculated parameters such as salinity, density and sound velocity at each depth. Analogous are the horizontal profiles obtained from CTD equipment mounted on towed bodies although the transit speed through the water is generally greater.

CTD data can also appear as a time series of values at fixed depths. These data, arising from moored instruments and typically sampled less frequently than profile data, rely on the motion in the ambient water to flush the sensors. Care must be taken in mounting the sensors and understanding their flushing characteristics to allow the measured parameters to be properly combined to produce accurate computed values of salinity and density.

CTD data is normally recorded digitally. In many commercially available instruments, an analog plot is produced either before (Bissett-Berman) or after (Guildline Mk IV) digitization but for large scale manipulation and computation of data, the digital recording format is almost essential. Plotted data is frequently the final output of the processing procedure and is often the best form in which to attempt physical interpretation but there is a necessity for digital computation and data storage in modern oceanography. In the following discussion it will be assumed that the CTD data is available in digital form and that sampling and recording of the sensor outputs has occurred at regular time intervals.

2. Instrumentation

Modern CTD instruments can record large numbers of rapidly sampled high resolution measurements. Table 1 is a short review of instrument specifications presently available. Two of the most advanced instruments, the Brown Microprofiler and Guildline Mk IV, sample at a rate of 25 or more times per second, while resolving temperature differences of the order of 0.0005°C and equivalent salinity differences of the order of 0.001. It is fair to assume that most CTD users will have been able to select an instrument giving them a sampling rate and resolution in excess of their needs. As modern electronics is adequately stable the limiting factors on CTD performance then become the sensor response characteristics and sensor calibration.

Calibration is not the direct concern of this study but it is important to mention in passing that conductivity cells in particular are subject to fairly rapid calibration changes and that frequent in situ checks of all three sensors are a necessity.

TABLE I

Characteristics of Commonly Used CTD's

Manufacturer and Model	Accuracy and (Resolution)			Data Rate Scans/s	Sensor Time Const. (ms)		
	Cond. (mS/cm)	Temp. (°C)	Press. (% F.S.)		Cond.	Temp.	Press.
Neil Brown Inst. Mk III	±.005 (±.001)	±.005 (±.0005)	±.1 (±.0015)	31	30	30	--
Guildline Inst. Mk. IV	±.005 (±.001)	±.005 (±.0005)	±.15 (±.01)	25	50	50	50
Inter Oceans Systems Model 660	±.005	±.005	±.2	10	20	60	25
Grundy Env. Systems Model 9051	±.02	±.02	±.1	10	15	350	20
Bissett-Birman Model 9040	±.03	±.02	±.25	2	100	350	100
Ocean Data Equipment	±.02	±.01	±.2	5	300	300	300
Acad. of Sciences, GDR	±.015	±.015	±.1	.83	350	350	100
Ozeanologische Messkette OM 75	(±.002)	(±.003)	(±.03)	1 (Averages)	630	630	630
Applied Microsystems CTD 12	±.005	±.01	±.1	.6	<100	<100	<100

N.B. The S.I. unit for conductivity is the Sieman, symbol S which is equal to a reciprocal ohm.

3. Sensor Response

Sensors should start to respond immediately to changes in the parameters they are supposed to measure. In the simplest case, a step change in say, temperature when experienced by the sensor produces an exponential rise in the measured value of this parameter. This idealized case is shown in Figure 1, curve A.

In practice, a number of other factors influence the shape of the temperature-time response curve. Sensors such as resistance thermometers, thermistors, etc. are usually surrounded by an electrically insulating layer that protects them from the surrounding water and are sometimes (unfortunately) closely connected to comparatively massive metallic bodies such as pressure cases, which materially affect their response. Figure 1, curves B and C are what might be expected from a temperature sensor showing these features. In comparison to curve A it is seen that there is an initial period where the response rises slowly, delayed by the time taken for diffusion of the step change through the protective coating of the sensor, and that there is a long "tail" while the response rises to its final value due to thermal conduction between the sensor and its support. We shall generalise the concept of time constant (which strictly speaking applies only to the simple exponential rise) and define it as that time taken for the response to reach 63% of the amplitude of the temperature step.

Cells to measure the electrical conductivity of sea water use two basic sensing methods: inductive and conductive. In the inductive sensor, the sea water is the medium linking two coils in a transformer and the losses associated with this linkage are measured to give a conductivity value. A typical configuration is a short cylinder containing coils pierced by an axial hole of diameter 1 or 2 cm; there is no direct electrical contact between the circuit and the sea water. In theory, the magnetic and electric field patterns of this sensor extend out to infinity, but in practice the conductivity measured is predominantly that of the water within the central hole. Nevertheless external bodies such as pressure cases, walls of laboratory tanks, etc. within tens of cms of the cell may affect its reading. This "proximity" effect makes them difficult to calibrate.

In a conductive sensor at least two, and usually four, electrodes are in direct contact with the sea water and these are typically contained within a glass or ceramic tube having a length of order cms to tens of cms and 0.5 to 1 cm diameter so as to provide a suitably high electrical impedence (100Ω) to the circuit. For example, the Guildline Mk IV CTD conductivity cell consists of a pyrex glass tube of internal diameter about 6 mm and length 14 cm, having four side arms containing the electrodes. The proximity effect is far less marked than for inductive sensors.

The time constants of these cells are primarily affected by the time taken for the water inside the tube to be exchanged, that is, they are "flushing" time constants, any delays due to the electrical circuitry usually being insignificant in comparison. The typical shape of a conductivity versus time curve for either of these conductivity cells responding to a sudden change in water properties is shown in Figure 2. The initial slow rise portion corresponds to the change approaching the cell, the steep slope to a change of water mass within the cell or between the electrodes, and the reduction to lower slope as the change moves away. In both cases there is a

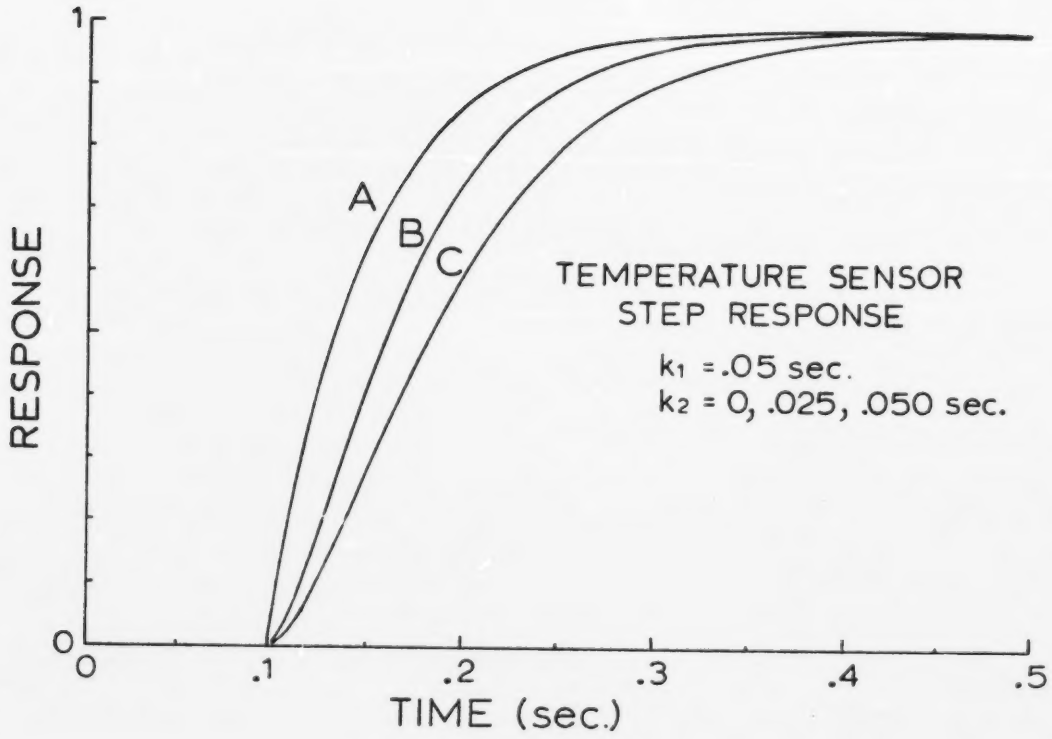

Figure 1. The response of a temperature sensor to a sudden change in the temperature of its environment. Curve A is the ideal exponential response. Curves B and C correspond more closely to reality for electrically (and thus thermally) insulated thermometers. k_1 and k_2 are defined in Appendix I. See text for discussion.

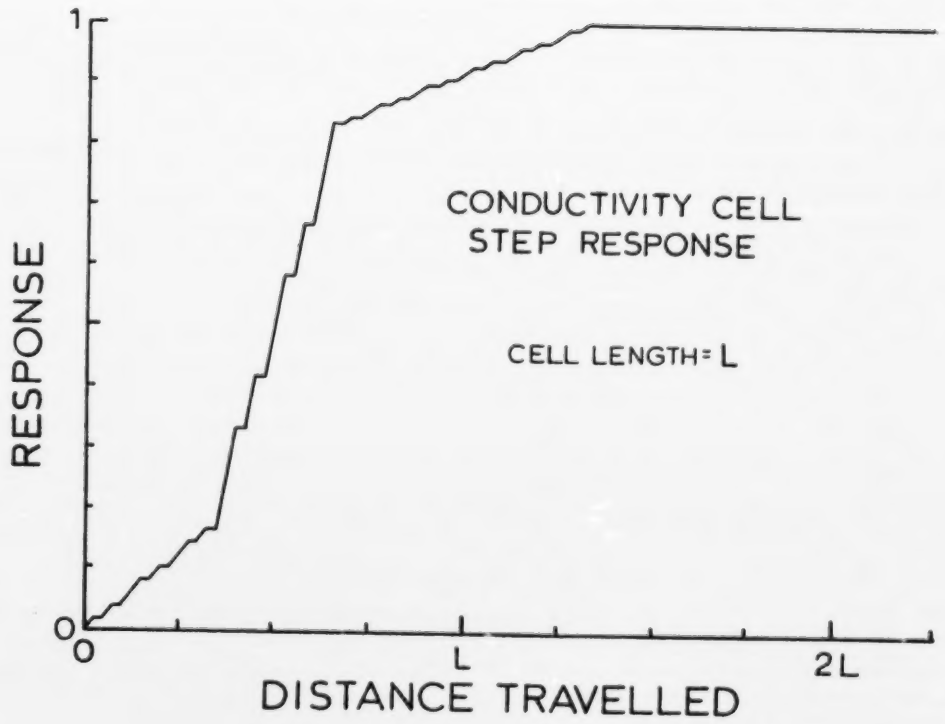

Figure 2. The response of a conductivity cell when lowered through a sudden change in that water property. The "stepped" nature of the curve is due to our finite interval technique of calculation; it would be smoothed out in practice. The three regions correspond to the water change interface approaching the cell, passing through the cell, and receding from it. The response reaches 63% of its final value when 0.55 of the cell length is immersed in the new water. See text for discussion.

long tail as it approaches the final value due to the boundary layer of "old" water remaining near the wall until flushing is complete. The proximity effect causes inductive sensors to have an effective length considerably greater that the physical length, far more than in the case of conductive sensors.

The preceding discussion of temperature sensor response considered an instantaneous change in the surrounding water mass. In practice, CTDs are being lowered through changing water characteristics and the speed of lowering plays a part in determining the temperature sensor time constant as it affects the fluid boundary layer next to the sensor and thus heat exchange with the water; also it controls the time taken for total immersion of a finite size sensor. However, the dominant factor is thermal conductivity. In contrast, for the conductivity cell the lowering rate is the most important parameter as it controls flushing; we can alter the time constant by altering the lowering rate. For both sensors the lowering rate changes a time constant into a distance reponse characteristic and so determines the maximum possible spatial resolution of the instrument.

Although the salinity calculation is not very sensitive to time constant effects in the pressure sensor, hysteresis problems can be important when the CTD is being lowered from a vessel subjected to major pitching and rolling which periodically alters the rate of descent. Under these conditions, the computation of the lowering rate from small pressure differences is usually made unstable by noise and resolution problems so that only greatly smoothed estimates of lowering rate can be obtained from the pressure record. These estimates are generally not good enough to aid in the reconstruction of small scale features through knowledge of the sensor response characteristics. The removal of unreliable data and low-pass filtering are frequently necessary in the presence of ship motion and the resulting loss of spatial resolution cannot be avoided. However, a knowledge of the time constants of all three sensors is of great importance in minimizing this loss and in making proper measurements of computed variables such as salinity.

4. Sensor time constant and sampling considerations

In the usual CTD lowering, temperature, conductivity and pressure are sampled and recorded sequentially. Depending on the electronics available, a set of values may be available up to 25 times per second; in other systems one complete scan of all three sensors takes more than a second. The factors of time constant, lowering rate and sampling speed are all interrelated in planning to obtain optimum salinity information and the discussion of these inter-relationships is the main subject of this paper.

To illustrate the problem involved first take the case of slow sequential sensor sampling at a lowering rate of 1 m/s so that the instrument moves a significant distance during one complete scan of the sensors. Figure 3 shows a sketch of the sensor positions on their protective cage beneath the CTD pressure case and defines appropriate geometric parameters. It is assumed that the sensors are sampled in the order pressure, temperature and conductivity. Very frequently sensors are mounted so that they are at the same horizontal level at any given time (i.e. $z = 0$) so that as the instrument is lowered through a sudden change in water properties the output of the temperature and conductivity sensors are not sampled when they are at the same position in relation to the discontinuity in water properties. For example, with a 1/3 sec interval between individual sensor sampling and a

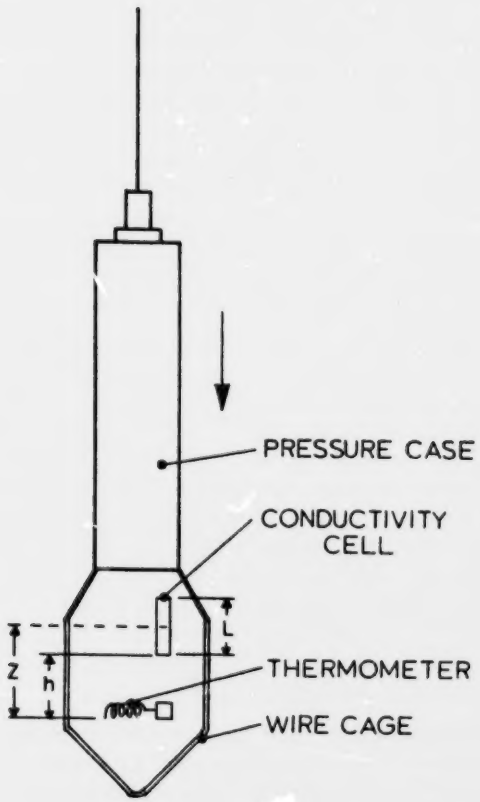

Figure 3. A schematic of the layout of sensors on the C.T.D. frame defining geometrical parameters used in the discussion.

1 metre/second lowering speed the sensor outputs are measured at positions 33.3 cm apart, so that in the presence of any gradients computed salinities do not give the value at either position. Therefore, even if the sensor time constant curves were identical, this sampling position offset could produce a major error in the salinity so computed.

As an attempted solution to the problem let the sensors be separated by 33 cm on the cage. The question now becomes one of whether their response curves are sufficiently similar. For example, if surrounding structures inhibit the easy flushing of the conductivity cell, so that it takes, say, 0.5 second to rise to 63% of its final value due to the water mass change, whereas the temperature sensor does this in 150 ms, it is clear that this could be interpreted as an additional separation between the sensors because their outputs would have reached different proportions of their true final values at the instant each electrical measurement was made. Even if the time constants were the same, differently shaped curves such as seen in Figures 1 and 2 would allow a different proportion of the change to occur in the same time.

The above discussion indicates one possible partial solution for sensor time constant differences; increasing or decreasing the vertical separation between the sensors around a central value dictated by the sampling interval. However, it must be noted that this is only good for one lowering rate; at 1 m/s, the 1/3 of a second interval was equivalent to a 33 cm sensor separation - at 2 m/s it corresponds to 66 cm. Most oceanographers work from ships, where, if the winch pays out cable at 1.5 m/s, the actual velocity of movement of the CTD fish may vary from 0.5 to 2.5 m/s according to the pitching and rolling of the vessel. Thus the appropriate separation for the sensors on the cage becomes problematical. Again, a "first-go" solution would be to determine the rate of pressure change with time from the data so collected, and to eliminate that data where the velocity of descent varied widely from 1.5 m/s, the undisturbed value.

As has been pointed out, the velocity of descent relates time constant to "distance constants" and a good point to enter the complex discussion of the optimum design of the sampling programme using a particular instrument with specified sensor characteristics, is to decide, a priori, what "slice thickness" of ocean is of interest in the particular study to be undertaken. For example, a typical oceanographic survey may require a value for every one m increment in depth in the surface layers changing to values for 10 m thick layers in deeper water. In this case it is essential that the recorded value typify that m or 10 m, not some particular turbulent swirl or step convection pattern that happens to immerse the sensor the instant the reading is taken. In other words, we must have a good system of averaging over the one or ten m depth intervals. To do this it is theoretically necessary to know the smallest scale temperature or salinity variations in the instrument's line of descent. These are transformed by the lowering rate into a maximum frequency which must be considered in relation to the time constants of the sensor. If the time constant is long compared to the period of their maximum frequency these variations will be severely attenuated. With a short enough time constant to leave the variations comparatively unattenuated the sampling rate must be adjusted to allow at least two samples in every period as a theoretical limit, 2.5 samples per period as a practical limit and 5 samples per period as a pessimistic limit. This is necessary to avoid problems due to "aliasing". A formal exposition of this problem is given

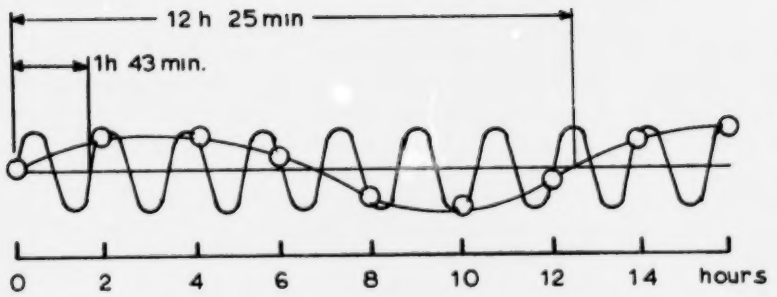

Figure 4. Aliasing illustrated. A sine wave of period 1 h 43 min is sampled every two hours which is interpreted by the observer as a wave of tidal period 12 h 25 min. The basic and minimum requirement in order that any sine wave should be assigned its proper frequency is a minimum of two samples per period, i.e. one sample per 51½ minutes in the present instance. After Sabinin (1967).

in Appendix II; a simple explanation is shown in Figure 4 adapated from Sabinin (1967). The effect of sampling at distance or time intervals greater than the periodic distance or time of the fluctuation is illustrated. The observer, knowing only the sampled values, concludes that a low frequency signal is present when in fact it is an artifact of the sampling technique applied to a higher frequency signal. "Power" has been shifted from high to low frequencies and the spectrum of the fluctuation of ocean properties so derived will be in error.

5. Computer Simulations of CTD Observations

To appreciate the complex interrelationships between sensor time constants and sampling rate, we shall consider the response to temperature and salinity profiles containing features designed for that purpose. Figure 5 shows this standard profile. Salinity is specified to vary linearly from S=15 in a uniform surface layer of depth 10 m to S=35 at 30 m and then continue with this latter value to the bottom at 70 m. The temperature decreases linearly for the first half of the salinity increase and thereafter oscillates at ever increasing frequency in the depth interval 20 - 40 m. The bottom 30 m is filled with steps of 1°C with the depth interval between steps halved for each successive step. It should be pointed out immediately that this profile is designed to explore the instrument characteristics and that in fact such an "ocean" is impossible in that the density of the water is not necessarily increasing with depth. Using the Practical Salinity Scale (1978) algorithms, the salinity and temperature so defined may be utilized to calculate the conductivity ratio of the water with respect to standard sea water of practical salinity 35 at 15°C and this conductivity ratio profile is also shown in Figure 5C.

The approach taken towards defining a time constant for the temperature sensor has already been illustrated in Figure 1. Curve A is a true exponential rise and corresponds to the idealized case of a sensor having no insulating coating responding to a step function increase in temperature. Curves B and C have been generated by a combination of two exponential functions which is discussed in detail in Appendix I, and are characterized by values of parameters k_1, k_2. The time constant of the idealized sensor k_1, remains at 50 ms but for curves B and C an increasing thickness of insulating material has been assumed to exist on its surface. For curve C, $k_2 = k_1 = k$ = 50 ms and represents a situation where the coating and the sensor are characterized by the same equation for temperature change with time. For a curve such as C, we have calculated the ratio between k and the time taken, τ, for the response following such a curve to reach 63% of its final value. k is approximately half this time constant (see Appendix 1). Each case must be considered individually but curve C does in fact seem to follow closely measured curves for certain thermistors, [Gregg & Meagher (1980)], and thermometers (Appendix I). Lastly, it must be noted that the time axis of Figure 1 is specific to k = 50 ms but that the abscissa scales directly with k so that curve C for k = 100 ms would see the values on the time axis doubled.

Figure 2 is used for simulating the response of the conductivity cell. The slope in the final portion of the curve is half that in the initial portion and this has been done in an attempt to simulate the slow removal of the boundary layer of "old" water within the cell as it is being replaced. The "stepped" nature of the curve is the result of calculating conductivity changes in finite increments and would of course be smoothed out in a real

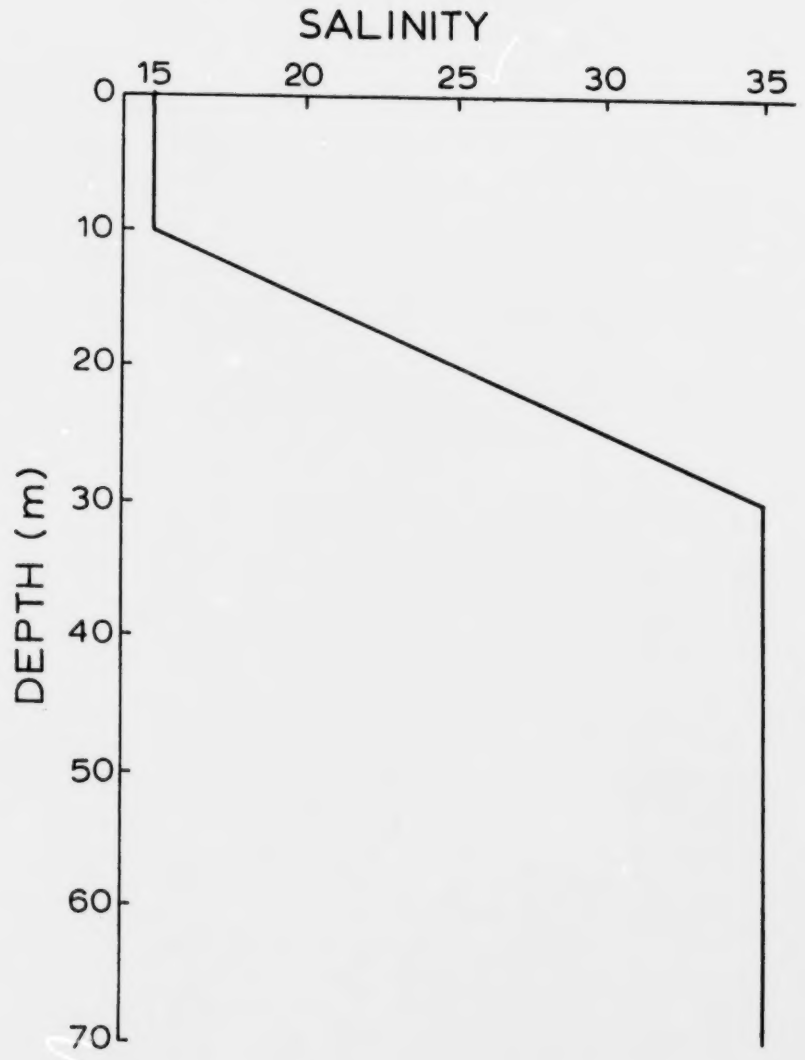

Figure 5A. Salinity profile specified for an artificial 70 m deep "sea". The "sea" contains a variety of features designed to explore fully, by computer simulation, the response of C.T.D. sensors "lowered" through it.

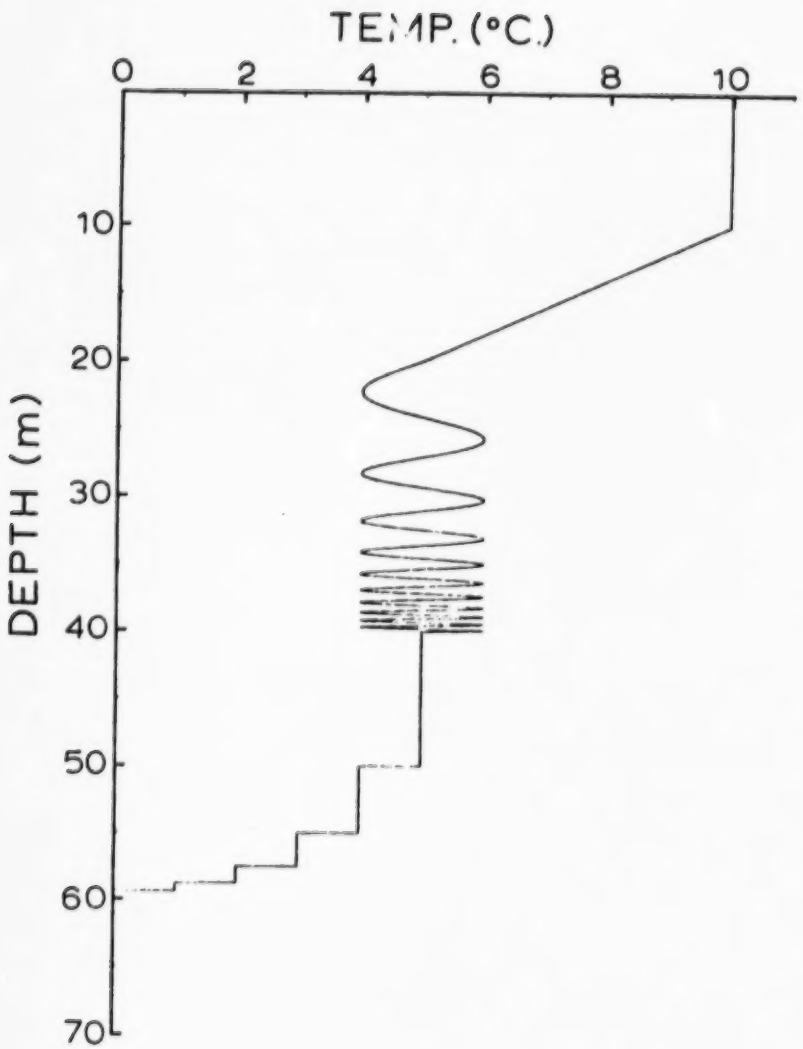

Figure 5B. Temperature profile specified for an artificial 70 m deep "sea". The "sea" contains a variety of features designed to explore fully, by computer simulation, the response of C.T.D. sensors "lowered" through it.

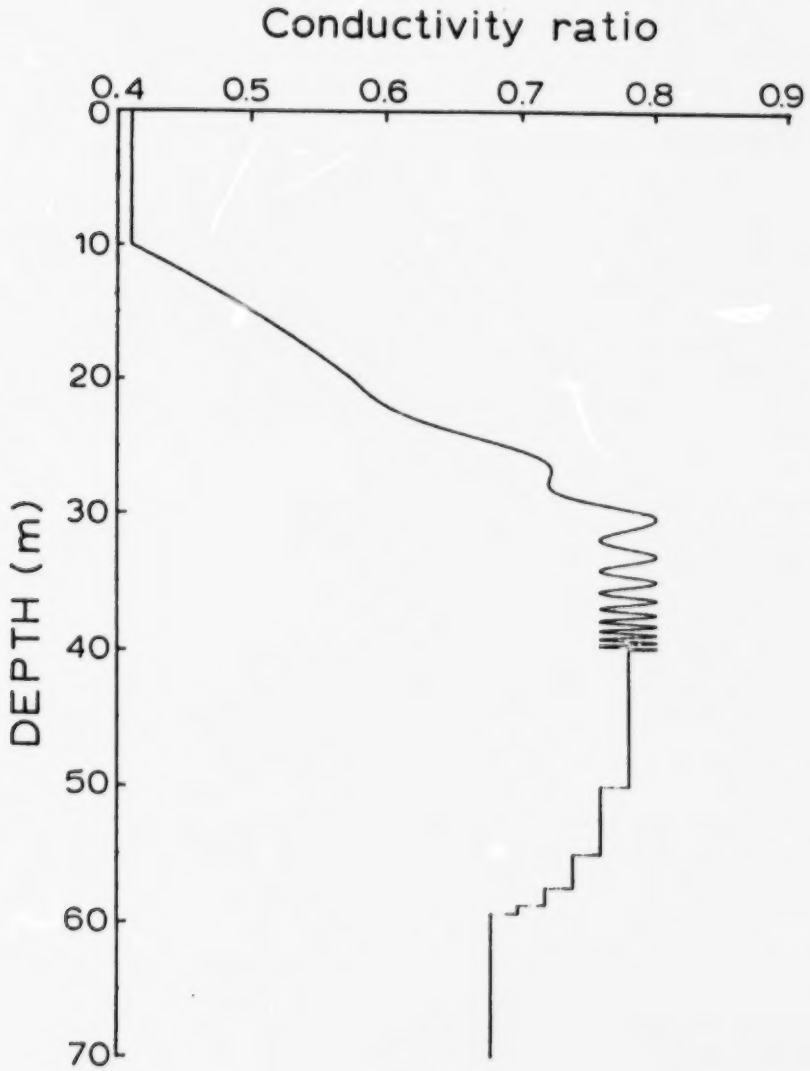

Figure 5C. Conductivity ratio profile specified for an artificial 70 m deep "sea". The "sea" contains a variety of features designed to explore fully, by computer simulation, the response of C.T.D. sensors "lowered" through it.

response. If CTD lowering were carried out at a 1 m/s rate and the cell were 10 cm long, Figure 2 shows that the response would reach 63% of its final value in about 55 ms. A 20 cm cell would take 110 ms, etc., etc.

Taking values typical of one of the older CTD designs, a cell length of 20 cm is paired with a temperature sensor with time constant ($\tau \sim 2k$) 200 ms. These two sensors are at the same level ($z = 0$ in Figure 3), are being lowered at 1 m/s and scanned once per second with 1/3s between the measurement of temperature and conductivity values. The standard ocean of Figure 5 appears as in Figure 6 to this instrument. At the given lowering speed temperature and conductivity sensors are approximately 33 cm apart at the time their outputs are being sampled, and when there is a change of salinity with depth, between 10 and 20 m for example, a salinity offset results due to the combination of temperature and conductivity readings from the two different levels. The level ascribed to the salinity so calculated is that of the depth of the centre of the conductivity cell. In the interval 20 - 40 m the temperature sensor endeavours to follow the sine wave but as frequency increases, an increasingly attenuated temperature signal results. In the end aliasing occurs, the high frequency is not resolved and spurious slow change in temperature appears. In the same interval the salinity has errors up to nearly 2. Large errors also occur where step changes in temperature have been imposed, for example at 50 m.

A first attempt to correct this state of affairs is to optimize the sensor positions in terms of their time constants, the lowering rate and the sampling frequency. It would be desirable that both sensors, when sampled, should have reached the same level of response to changing values in the ocean. As the two response curves are differently shaped, this can only be made to be true exactly at one point. Rather arbitrarily we will select the instant at which they have reached 63% of their final value, that is one time constant after the start of a step change. Suppose the sensors were sampled simultaneously. The distance moved by the probe during the time for the temperature sensor to reach 63% of its final value is τv, where v is the lowering speed of the instrument. If, at this time, the conductivity sensor has reached the same percentage response approximately 0.55 of its length will be immersed in the new field so that we may write the equation (Figure 3 defines h and L).

$$h = \tau v - 0.55\ L$$

However, sampling is not usually simultaneous but separated by a time interval δt and we will assume that this quantity is positive if the temperature sensor is sampled before conductivity. A further distance $v.\delta t$ between the sensors must be introduced to compensate for this interval so that the total distance h from the bottom of the conductivity cell to the temperature sensor can be expressed as

$$h = v(\tau + \delta t) - 0.55\ L \qquad (1)$$

This arrangement should match this response of the sensors at one point, the 63% value, but if it is possible to control v, the lowering speed, a match at a second point is possible. With the temperature sensor a distance h in front of the conductivity sensor there is a distance $h - v.\delta t$ when only one sensor will have responded to the step change. Should sampling occur in this interval, major errors will result. Ideally it should be set to 0 which is

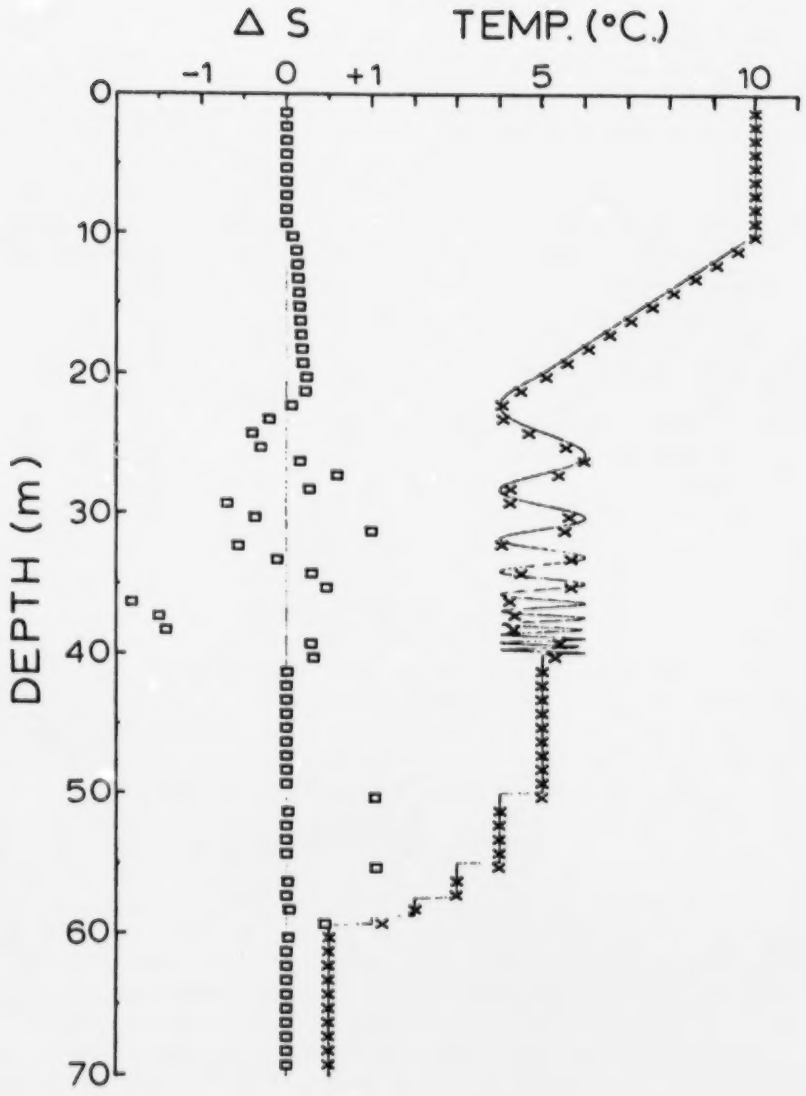

Figure 6. Our "sea" (Figure 5) as seen by a C.T.D. having a 20 cm long conductivity cell and a 200 ms time constant thermometer at the same level (i.e., z = 0 Figure 3) when lowered at 1 m/s and completely sampled once per second (1/3 sec. between individual conductivity and temperature values). ΔS is the difference between the individual computed salinity values (squares) and the true values of the "sea". Crosses show the measured temperatures, the continuous line being the true "sea" temperature.

equivalent to making both sensors match at the start of their response as well as at the 63% level. In this case, $h = v.\delta t$ and v is defined by

$$v = 0.55\ L / \tau \qquad (2)$$

Using the dimensions as for Figure 6 as an example, this would give a lowering rate of about 55 cm/s.

Figure 7 shows the result of applying equation (1) to our standard ocean investigated by the same sensors. It is immediately noted that there is a great improvement in the salinity scatter and that the offset, both in temperature and salinity, in the interval 20 - 40 m has been eliminated. The attenuation in the temperature signal at increasing frequency occurs as before, with aliasing between 35 - 50 m. The slow speed of sampling means that there is some arbitrariness in the errors occurring at the steps below 40 m as they depend on when the assumed instantaneous sensor sampling occurs in relation to traversing the step. Figure 8 is the result of applying both equations (1) and (2) to the same sampling. The velocity of descent is now 55 cm/s, not 1 m/s, which means that there are more samples per metre at the fixed sampling rate of 1 scan per second. Although it is not obvious from the figure the salinity errors have once again been decreased. A printer output shows that the maximum error recorded while the instrument traverses the temperature steps has dropped from 0.14 to 0.04! It can also be seen that the increased density of sampling with depth has improved the aliasing situation in the 35 - 40 m interval. Only the highest frequencies are now aliased.

Further insight can be derived from looking at the results of fast sampling using the same sensors. We have considered 25 scans per second and the application of equation (1) in producing Figure 9 which illustrates the performance of such a CTD in the depth interval 20 - 40 m in our standard ocean. Aliasing is no longer present though the higher frequency portion of the sine wave becomes severely attenuated by the slow response of the temperature sensor. A considerable degree of salinity noise is present at these higher frequencies which, as mentioned above, is due to there being an interval $h - v.\delta t$ where the temperature sensor will have started to respond to the change without the conductivity sensor having yet "felt" it. Figure 10 shows the reduction in salinity noise brought about by applying both equations (1) and (2) to the same sensors. As the lowering speed has dropped from 1 m/s to 55 cm/s the attenuation of the sine wave had been materially reduced due to the temperature changes being sensed at a lower frequency and the remaining salinity noise is now primarily due to the difference in shape between the temperature and the conductivity sensor response curves which we have forced to agree at the 0 and 63% values. This represents just about the best it is possible to do with the instrument. If one wishes to resolve these high frequencies a faster time constant is required.

A further illustration of the difference in salinity readings obtained by applying equation (1) alone, or (1) and (2) simultaneously and thus fixing the descent velocity is given in Figure 11 which illustrates response to the temperature discontinuity at 50 m in our standard ocean at various lowering rates. In going from the fastest to the slowest lowering rates $h-v\delta t$ goes from being positive to negative through zero at the optimum lowering rate of 55 cm/s fixed by equation (2). Thus at the fastest rates

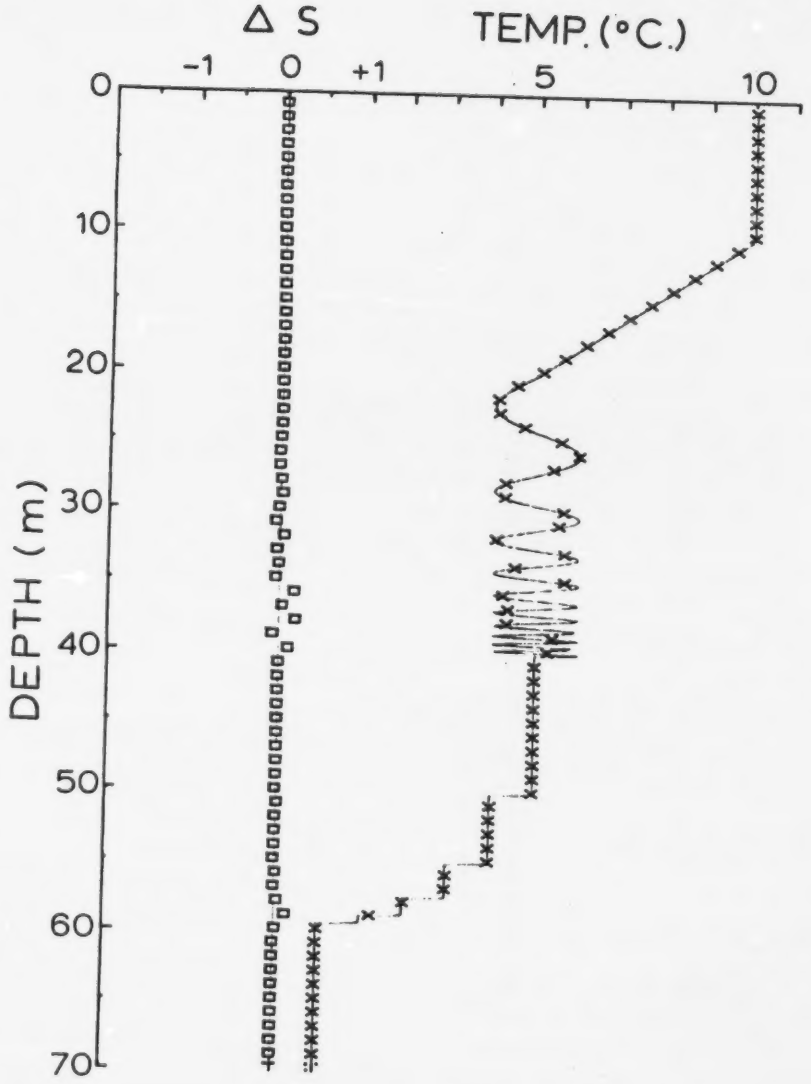

Figure 7. Our "sea" (Figure 5) as seen by a C.T.D. as described in the legend for Figure 6 but having the value of the sensor separation (z in Figure 3) set by equation (1). ΔS is the difference between the individual computed salinity values (squares) and the true values of the "sea". Crosses show the measured temperatures, the continuous line being the true "sea" temperature. Note the greatly reduced errors in salinity values as compared to Figure 6.

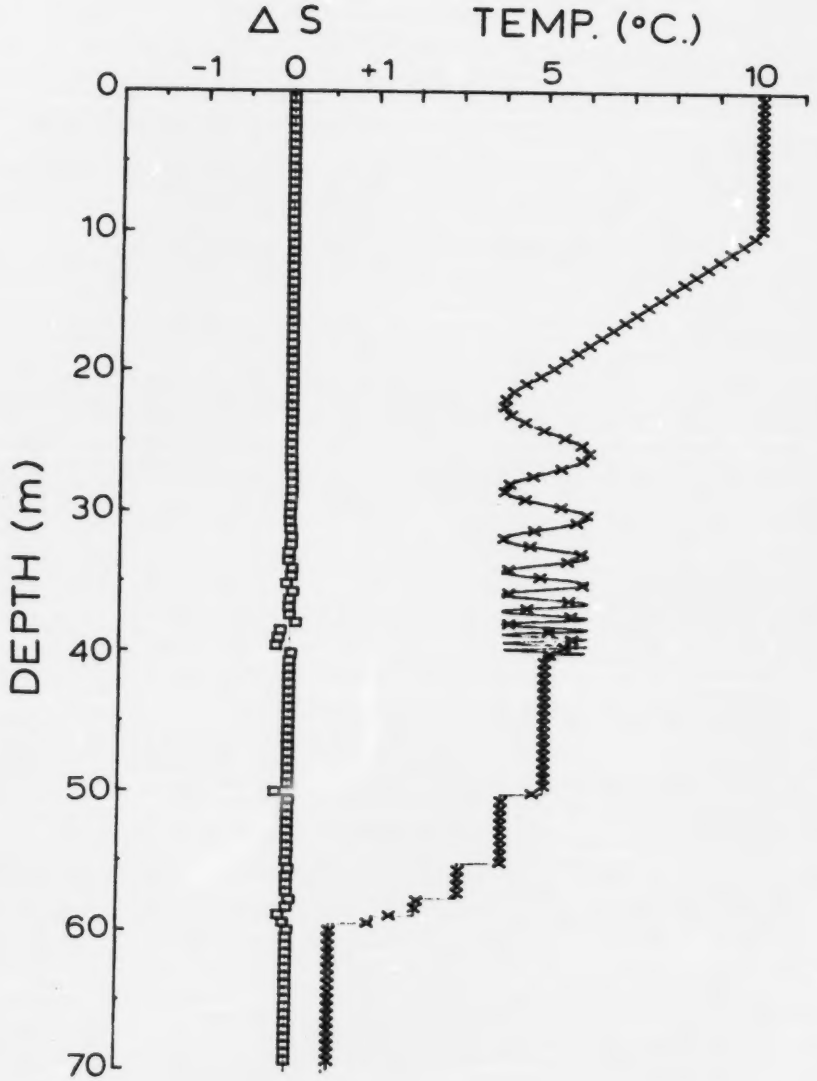

Figure 8. Our "sea" (Figure 5) as seen by a C.T.D. as described in Figure 7 legend but with the optimum lowering rate determined by Equation (2) to be 55 cm/sec. This nearly doubles the number of samples per meter compared to the previous figures and produces an improvement in both ΔS and temperature. ΔS is the difference between the individual computed salinity values (squares) and the true values of the "sea". Crosses show the measured temperatures, the continuous line being the true "sea" temperature.

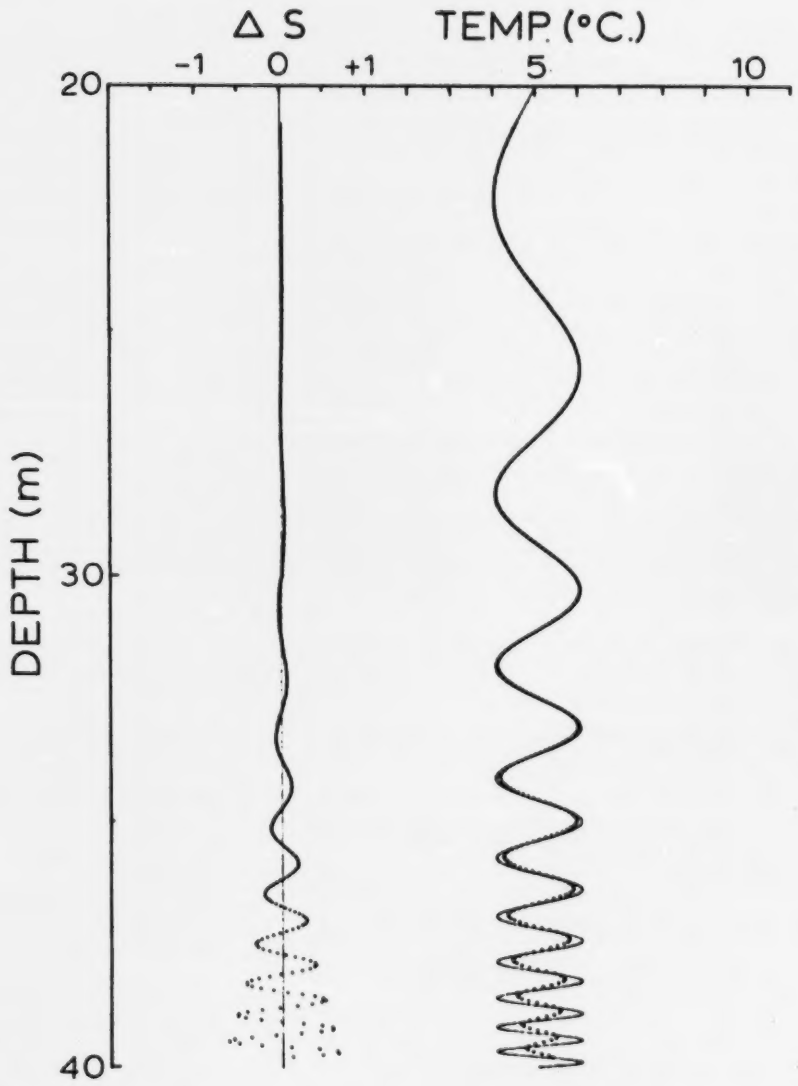

Figure 9. An expanded view of the 20 - 40 m section of the standard "sea" as seen by the C.T.D. described in the legend of Figure 7, but with sampling 25 times per second instead of once. The Equation (1) constraint has been applied. Each measurement is a dot, the continuous line gives the true value. Lowering speed is 1 m/s.

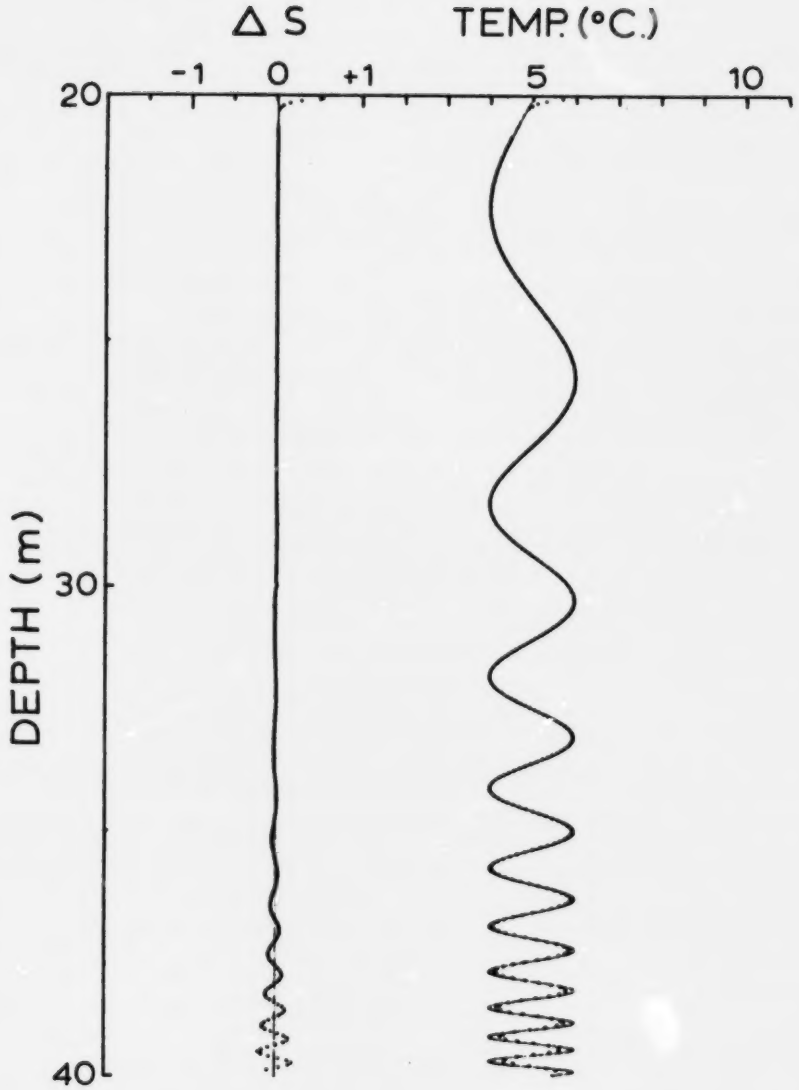

Figure 10. Detail as in Figure 9 but with the Equation (2) constraint applied as well to Equation (1). This drops the lowering speed to 55 cm/s. Note the great improvement in the salinity representation. See text for discussion.

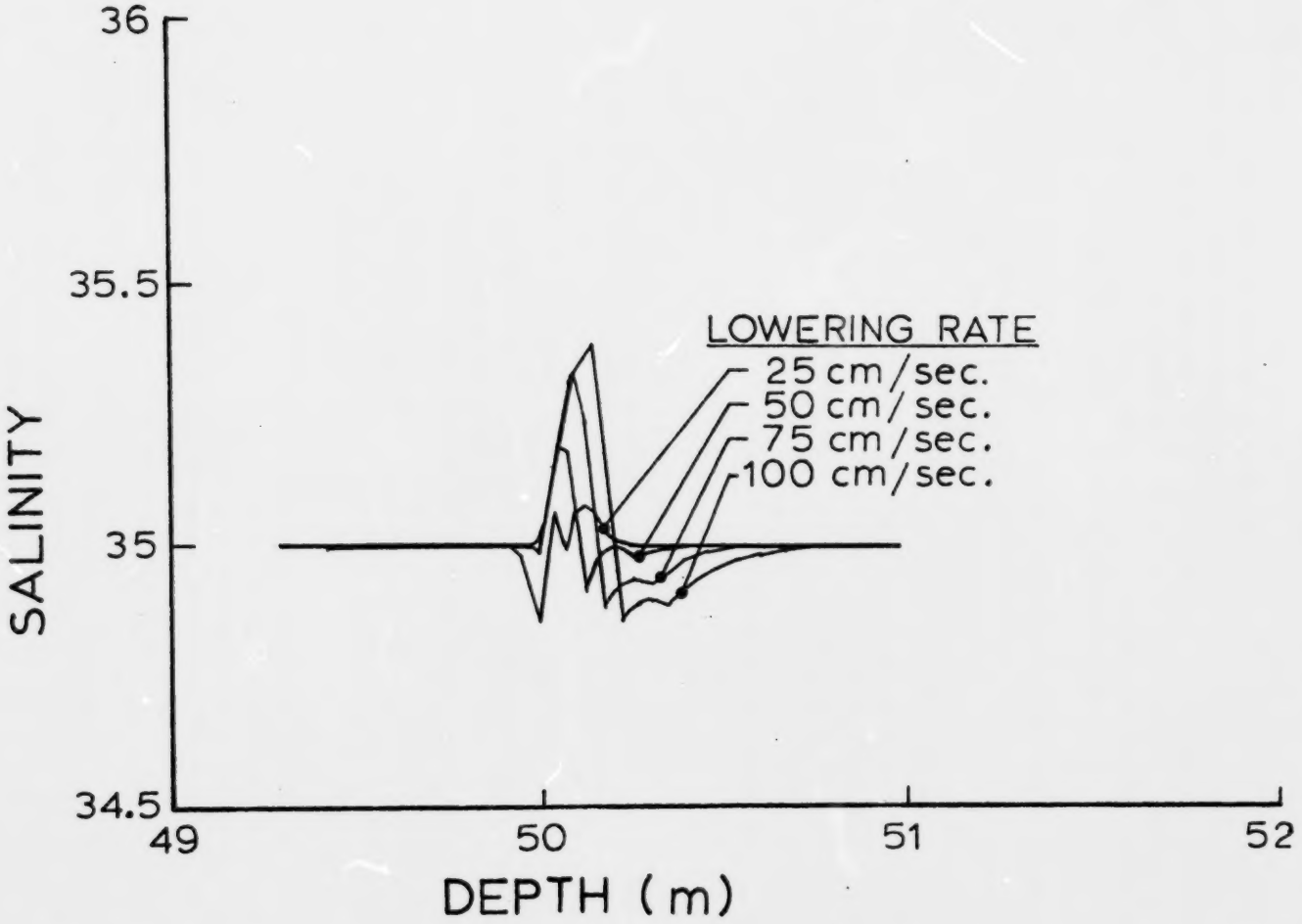

Figure 11. The effect of lowering rate on the salinity spike caused by the temperature step at 50 m depth in the standard "sea" (Figure 5B). Equation (2) gives the optimum lowering rate at 55 cm/sec. and it may be seen that the 50 cm/sec rate does make the distortion more or less symmetric and minimal.

the temperature sensor starts its response before the conductivity sensor. At the lowest rates the opposite is true. The optimum constitutes a balance between the two effects minimizing the salinity swing on either side of its correct constant value.

If the exact response of the sensors is known and measurements such as are shown in Figures (6) and (7) are available it would be possible to attempt a "recreation" of the real ocean temperature and conductivity profiles based upon this information by inversion techniques. Unfortunately it is likely that numerical instabilities arising from small errors and insufficient sampling (Fofonoff, Hayes and Millard (1974), and Middleton and Foster (1980)). will cause salinity errors equal or greater than those shown in Figure (7).

6. Application to field observations

The principles laid down in the preceding chapters will now be applied to field data. Data acquired from ships frequently shows large fluctuations in the velocity of descent of the CTD but that acquired from the sea ice surface has usually been obtained at a constant velocity. The latter data is considered first as a simple case. Figure 12 shows sections from two CTD profiles from the Canadian Beaufort Sea taken in November/December 1979. Both sets of curves show the temperature profile and the salinity as calculated for various values of τ as defined for use in equation (1). The instrument was Guildline Mk IV CTD with a thermometer time constant of 50 ms as given by the manufacturer ($k \simeq 25$ ms) and a conductivity cell length of 14 cm. From the pressure sensor readings it was determined that the instrument was lowered at a speed of 1.5 ± 10% m/s. The sensors are mounted on the instrument so that z = 0, i.e. 7 cm of the vertically mounted conductivity cell are on each side of the axis of the thermometer, a helical coil, which is horizontal during a vertical descent. The sensor outputs were sampled 25 times per second, and there was a delay of 5 ms between the sampling of the temperature and conductivity sensors (δt = 5 ms).

At this fast sampling rate it is not necessary to physically move the sensors with respect to each other as illustrated in Figure 3. The water mass properties have been taken every 6 cm during the descent, and as neither sensor will respond significantly to fluctuating water properties at a smaller length scale, the time series of temperature and conductivity values may be considered smooth for interpolation purposes. The temperature and conductivity values to be combined to give a salinity are then selected from their time series so as to be separated by a time interval h/v, which is equivalent in this case to an actual physical separation of h. This procedure of "slipping" the time series is far more convenient as for a given δt one would have to alter the value of h for each new value of v, were it necessary to achieve the desired effect by actual sensor separation. For slowly sampled instruments, for example those having a second between samples as used to produce Figure 6, an actual physical separation is necessary as the sensors could respond significantly to unresolved fluctuations in the water mass properties during that interval.

Figure 12A shows the remarkable improvement obtained by applying equation (1) each profile being characterized by a particular value of τ. It is seen that τ = 50 ms produces by far the smoothest result and that quite a number of "significant features" in the salinity profile have been eliminated by this processing technique. In an environment with a smoothly changing salinity/depth profile, major temperature fluctuations, combined

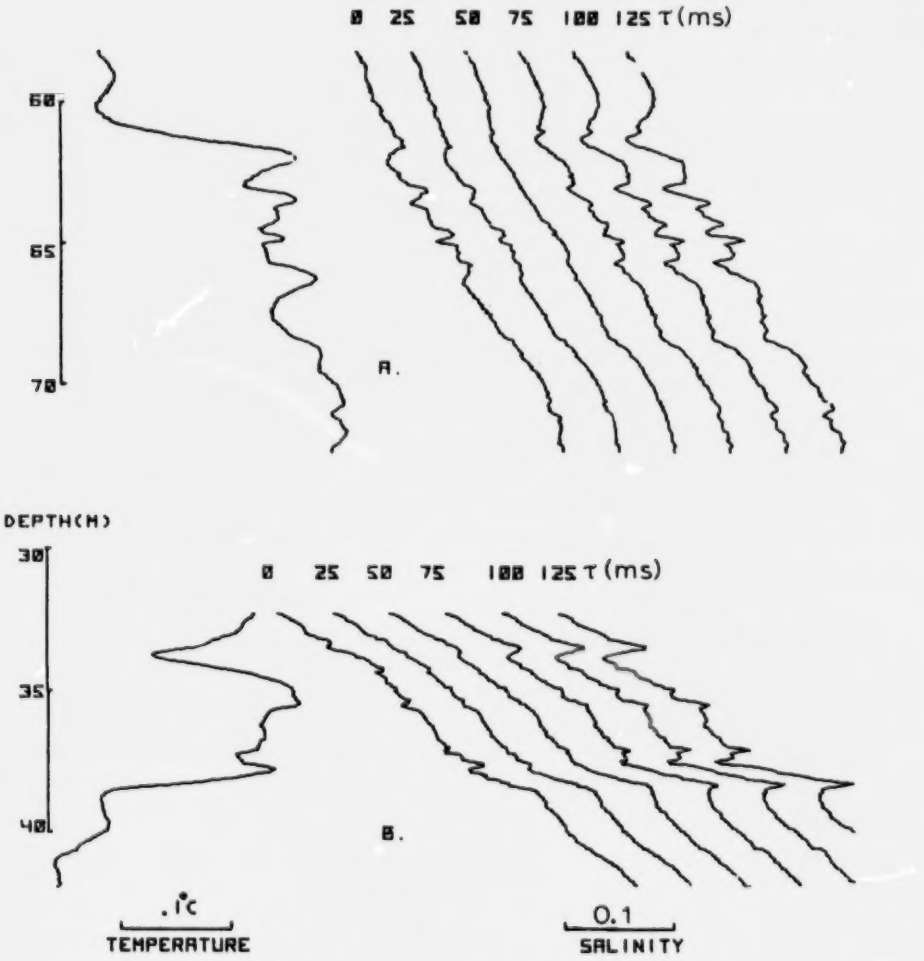

Figure 12 A and B. The processing of two sections of data from the Beaufort Sea. In both cases the salinity is increasing steadily with depth but temperature, the left hand curve in both cases, has considerable structure. The set of six curves on the right are labelled with the values of τ taken for the computation of salinity using Equation (1) to move the temperature and conductivity ratio time series in relation to each other. It is seen that most of the salinity structure is removed by taking τ = 50 ms, which is the manufacturer's given value. It is interesting to note the spurious "intrusive layers" created by taking other values.

with conductivities taken at the "wrong time" have produced artificial salinity changes. It is important to realize that these spurious features have been simply generated by allowing a variation of τ from 0 to 100 ms. Figure 12B illustrates the well-known phenomenon on "spiking" at sudden changes in the slope of a temperature or conductivity curve, and its elimination by proper processing.

The question does arise of how the curve for τ = 50 ms is selected as being "best". It is noted for example that the feature at the 65 db pressure level on Figure 12A has very noticably reversed its direction to turn from a salinity reduction to a salinity increase as the value of τ is increased, and is flattened out at τ = 50 ms. This would be typical of transiting the correct value as a temperature taken too soon for the appropriate conductivity reading was transformed into one taken too late. On Figure 12B the spikes of temperature and salinity at about 38 db are certainly associated with each other and the use of τ = 50 ms has resulted in the elimination of the salinity spike. Nevertheless, it must be admitted that some subjectivity still exists in the argument, which is one of the reasons why the criteria were applied to a known computer-generated ocean in the preceding chapter.

The next logical step would be to apply equation (2) to the τ = 50 ms curves of Figure 12 to see if a further improvement to this data would result. On putting appropriate values into equation (2) it is found that an optimum value for the descent velocity would be 1.54 m/s so that the difference between this ideal rate and that actually used in practice is too small to make any significant difference in the result. In other words the Guildline Model Mark IV used at 1.5 m/s is a very well balanced piece of equipment!

In shipborne use, where the velocity of descent of the probe may go through large and sometimes violent fluctuation, including reversal, this simple approach cannot be expected to compensate for the complicated fluid dynamical processes which result. It is best to specify a range of lowering rates and data outside these limits which can be excluded from processing or flagged to indicate their lower expected accuracy. The remaining data can be processed as described above.

This was done for two stations taken during Discovery Cruise 81 by the Institute of Oceanographic Sciences, Wormley, U.K. in January 1980. The instrument used was a Neil Brown CTD equipped with a 200 to 250 ms time constant temperature sensor. The conductivity sensor, whose effective length is about 3 cm, responds much more rapidly than the temperature sensor and this difference must be reconciled in data processing. The velocity of descent of the probe varied between 12 cm/s and 175 m/s as the data shown in Figure 13 was collected. Figure 13A shows the results obtained by application of equation (1). The features at 665 and 690 db pressure are responding to the changes in τ and appear to reach a minimum at τ = 250 to 300 ms. Figures 13B shows the results of the application of equation (2); i.e. filtering of the conductivity as parameterized by the expression 0.55 so as to artificially increase time constant. As is seen from the equation the filtering required is a function of velocity of descent so that the filter is continuously varying. Details are given in Appendix I. Note the general loss of detail and the smoothing of sharp features such as the step at 660 db pressure as this artificial time constant is increased. For this reason, it is difficult to make an objective assessment of the quality of the profiles but τ = 275 ms appears to be close to the optimum.

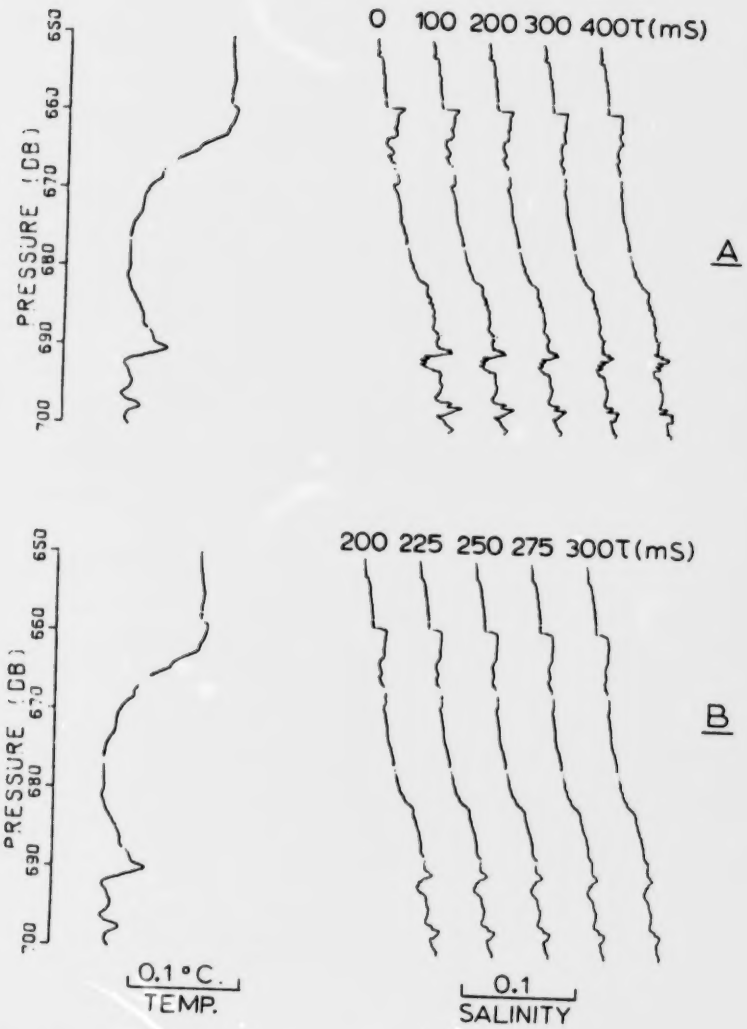

Figure 13 A and B. Processing of section of data collected by I.O.S., Wormley, U.K. The velocity of descent varied from 12 cm/sec to 175 cm/sec during this record. The range 200 ms $<\tau<$300 ms is selected from A as optimum for adjustments based on Equation (1) of text, and then applied to produce a filter for the conductivity sensor data with the result shown in B. Temperature profiles are given on the left. All values taken when the probe was moving at less than 50 cm/sec have been eliminated from the record.

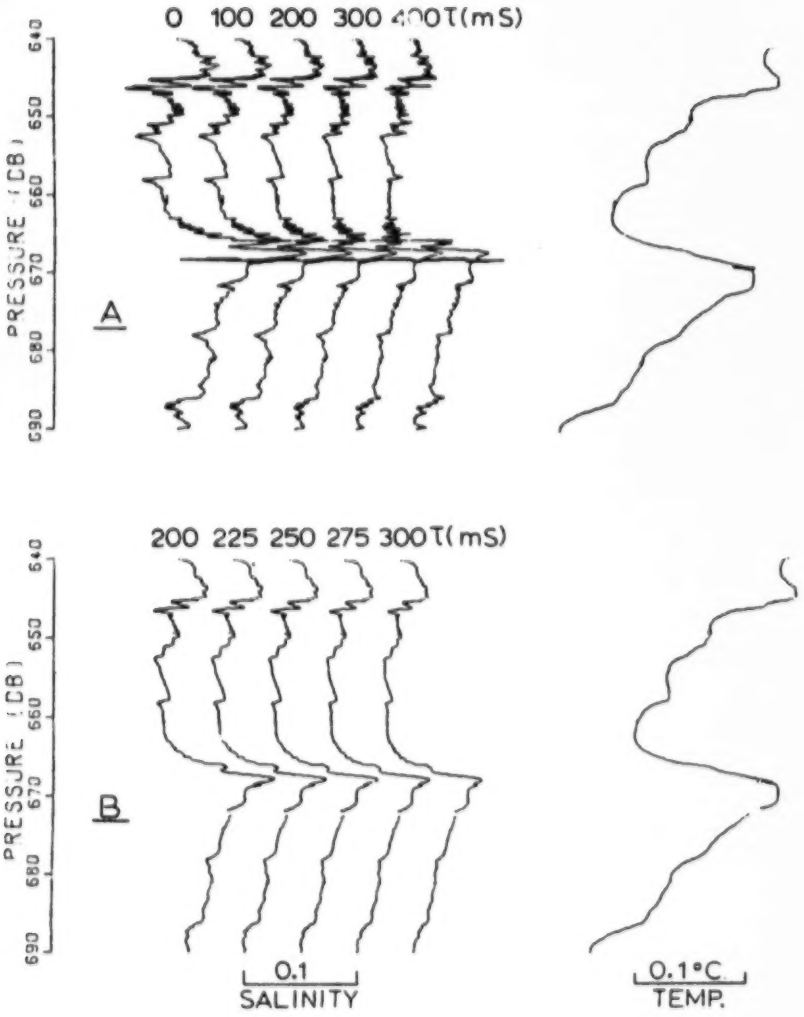

Figure 14 A and B. Processing of I.O.S., Wormley data having negative probe lowering rates due to violent ship movement. Section A shows all the data and the application of Equation (1) allowing selection of τ within range 200 to 300 ms. Feature at 669 db caused by velocity reversal. Section B shows application of Equation (2) and elimination of all values taken when probe was moving at less than 50 cm/sec. Temperature profiles are given on the right.

Figures 14A and 14B show the same procedure done to a profile with a more violently changing lowering rate (2·25 m/s to -40 cm/s in 4 m) in a section of water with greater temperature gradients. In Figure 14A, many of the high frequency salinity features seem to come about in the presence of high temperature gradients independent of lowering rate variations. These arise mainly out of the time constant mismatch and are largely damped out in the second stage of processing, Figure 14B. Some features such as the spike just above 670 db arise from negative lowering rates (in the presence of a temperature grandient) and are deleted by ignoring all data taken below a 0.50 m/s lowering rate which has been done in Figure 14B, where the varying filter of equation (2) is used.

Features of questionable validity such as at 645 db still survive. Nevertheless, the τ = 275 ms curve still seems to produce the best result. This serves to demonstrate the limitations of this kind of processing which produces an optimum profile to be viewed critically before being accepted. In practice it is generally agreed that all CTD data taken with negative portion to the probe velocity cycle is of little use. Water is dragged along by the probe which is engulfed by this wake as it rises and it appears impossible to place bounds on the precision or accuracy of the data. In this case, the effect of the processing scheme on the salinity profile of Figure 14 has been to change the computed salinity (10 m average) by up to 0.0006 depending on the temperature gradient. Effects of this size can have a large influence on stability calculations.

7. Further data processing

A less elaborate form of the procedures outlined in the previous chapters have been suggested frequently in the literature. Often combined with averaging to further reduce the "bumps".

Probably the nearest approach to our suggested procedure was given by Roden and Irish (1975) who assumed that both temperature and conductivity sensors obeyed a simple exponential response law (as shown in Figure 1A) and made corrections for the difference in time between the sampling of their two sensors and for different values of the time constant. The proper value of the parameter to be used for the salinity calculation was arrived at by an equation of the form

$$P_{Measured} = P_{True} - k\frac{\partial P}{\partial t}$$

where P is the appropriate parameter. It will be seen that a match of the two response curves at one point only is possible by this procedure, unlike the two point match that we have suggested. The authors find a suitable value of $\partial P/\partial t$ by a simple finite difference approximation taking successive values as recorded. This tends to leave considerable noise in the system. Other authors have used more elaborate schemes for finding $\partial P/\partial t$ but have usually assumed that the response of the conductivity cell is instantaneous. For example, Fofonoff, Hayes, Millard (1974) use a least squares fit of the temperature time series to extrapolate it forward a time equal to the time constant before combining this value with the conductivity measured at the time.

After computing salinity many authors have suggested further processing of the data to remove noise and any other features left over from imperfections in salinity calculating schemes such as have been discussed above. In particular, there are a variety of proposals for the elimination of "spikes" that frequently occur at places in the ocean where the slope of a parameter changes discontinuously. Also in this category come "wild values" generated by momentary failures in the equipment, reception of extraneous electrical pulses, etc. The description of one of the most elaborate of these schemes will serve to suggest them all. It is due to Acheson (1975). The first thirty values of the time series of the parameter are taken and fitted to a second-degree polynomial by a least squares method. Values deviating from this fit by more than three standard deviations are flagged. Fifteen more values are taken and combined with the second half of the previous thirty. A new fit is made, and once again those values differing from the curve by more than three standard deviations are flagged. Any point which has been flagged from both fits is discarded and replaced by a value computed from the coefficients of the least squares fit. The next fifteen points are shifted into the scheme and the above procedure repeated.

Obviously common sense must also be used; if the thirty points chosen span a depth at which there is a sudden change in slope of the parameter (such as the bottom of a mixed layer) a quadratic fit to those thirty points is not good enough and a number of points that are in fact correct will exceed three standard deviations from a curve so computed. Nevertheless, it is a very effective technique for removing random errors and any spikes remaining from imperfect corrections in salinity calculations and is recommended.

Another form of data averaging is to record only the average value of N readings in an attempt to typify the value of the parameter over the depth interval corresponding to $N\Delta t$ where Δt is the scan interval. This procedure reduces aliasing by averaging out unwanted rapid variations and allows more compact data storage than recording each reading. It can, however, seriously reduce the ability to correct for time constant mismatches. This is because these errors are proportional to the gradients encountered in the water column, particularly if strong gradients occur over time scales roughly equal to the time constant of the sensor. If averaging spans a time of one time constant or less ($N\Delta t<\tau$) then these gradients can still be found in the data and sensible corrections can be made. However, if averaging has been done over a number of time constants ($N\Delta t>\tau$), these rapid variations will have been lost making estimation of errors due to time constant mismatch impossible. In the extreme case of an averaging period being equal to many time constants ($N\Delta t>>\tau$), no corrections would be necessary because of the complete masking of any sensor inertia by the inertia of the averaging process. Another way of viewing this effect is to say that the averaging process severely attenuates the high frequency variations which are affected by time constant. It is important to realise that the maximum frequency detectable by the sampling scheme is the Nyquist frequency ($1/2N\Delta t$). (See Appendix III.).

Data of this form is best handled by the normal time constant compensation routine recommended in Appendix 1. It becomes less and less effective the longer the averaging period and is unnecessary for extremely long averaging periods. For moderate averaging periods greater than one time

constant, the problem can be averted by matching time constants, for example, by careful control of lowering rates.

Appendix I - Sensor time constants and adjustments

In its simplest form a sensor responds at a rate proportional to the difference between the environmental values of the parameter to be measured and the current values of that parameter taken on by the sensor. A typical example of this behaviour is a temperature sensor, the heat flow into which is proportional to the temperature differences between the sensor and environment. The temperature registered by the sensor changes at a rate proportional to this heat flow, thus:

$$\frac{\partial T_s}{\partial t} = (T - T_s)/k \qquad (1)$$

giving

$$T_s = 1 - e^{-t/k} \quad (t>0)$$

if $T = 0$ for $t<0$

$T = 1$ for $t \geq 0$

T_s = sensor temp.

T = environment temp.

k - constant of proportionality

The constant of proportionality is called the time constant and is an often quoted parameter in sensor specifications. More generally, and in this paper, the time constant is the time taken for any sensor to rise to 63% of its response to an abrupt change in water properties.

A more detailed look at the way sensors are constructed and mounted reveals some of the causes of deviations from the above response characteristic. In particular, the protective coating surrounding temperature sensors delays the initial response while the heat from this layer is dissipated. This behaviour has been determined for glass coated thermistors by Gregg and Meagher (1980) who also studied the effect of the fluid boundary layer in the heat diffusion process. They found that the sensor response was best fitted by a double time constant system. The two time constants could not be separately calculated from their data, but a good fit to the measured response was obtained from setting the two equal to each other. This type of response curve can be explained by the following simplified model. Consider the coating to be coupled to the outside environment through one time constant, k_1;

$$\frac{\partial T_c}{\partial t} = (T - T_c)/k_1 \qquad (2)$$

T_c = temperature of coating

and the temperature sensing element to be coupled to the coating through another time constant k_2;

$$\frac{\partial T_s}{\partial t} = (T_c - T_s)/k_2 \qquad (3)$$

Combining equations (2) and (3) to eliminate T_c;

$$k_1 k_2 \frac{\partial^2 T_s}{\partial t2} + (k_1 + k_2) \frac{\partial T_s}{\partial t} + T_s = T \qquad (4)$$

If T is a step input: $T = 0 \quad t<0$
$T = 1 \quad t \geq 0$

$$T_s = 1 - A(e^{-t/k_1} - \frac{k_2}{k_1} e^{-t/k_2}): \quad A = 1/(1-k_2/k_1) \qquad (5)$$

or, if $k_1 = k_2 = k$

$$T_s = 1 - (1 + t/k)e^{-t/k} \qquad (6)$$

An example of this kind of response is plotted in Figure 1C.

The response of an oceanographic copper resistance thermometer protected by a stainless steel sheath is shown in Figure 15 along with the fitted response given by equation (6) with k = 55 msec.

Other factors modifying the response of oceanographic temperature sensors are:

1. Thermal coupling to the pressure case which results in a portion of the sensor response taking on the slower time constant of the case.
2. Velocity scaling of the time constant through modification of the fluid boundary layer thickness. Gregg and Meagher (1980) found that the maximum frequency detectable by their thermistors scales as $v^{1/3}$ where v is the speed of the sensor through the water. Walker (1978) includes the velocity dependent immersion time of a 4 cm dia. temperature sensor.
3. Entrainment of water in the wakes of shrouds and mounting hardware. Goulet and Calverhouse (1972) describe a problem of this sort encountered on a Bisset-Birman 9006 STD and Paige (1978) describes the effect of mounting angle for the NBIS Mark IV CTD thermistor. Millard, Toole and Schwartz (1980) describe an alternate recording scheme in order to optimize the retrieval of high frequency temperature data for this instrument.

All of these problems should be solved in hardware before any data is taken. The following solutions are offered as examples:

1. A thermally insulating spacer between the sensor and the pressure case should be included in the sensor mounting.

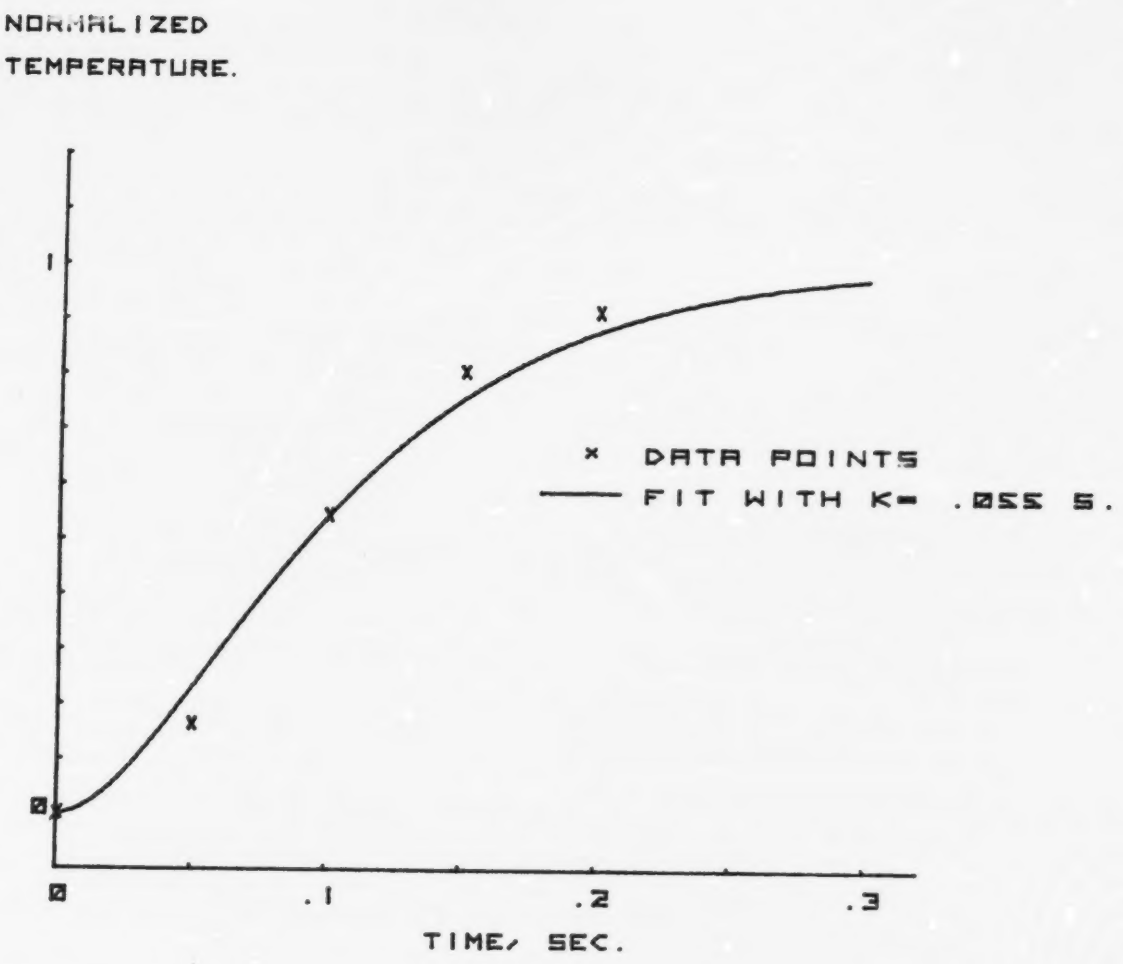

Figure 15. The response of an oceanographic temperature sensor fitted to a double time constant curves ($k_1 = k_2 = .055$ sec).

2. As much as possible, the CTD should be lowered at a constant rate so as to minimize the velocity modulation of the response characteristic.

3. Care should be taken to allow free flushing of the sensor. Frequently, water tunnel test results as well as other information for particular instruments are available in the NOAA Instrument Fact Sheet and NOAA Technical Memorandum Series.

Conductivity cells can be modelled in a very rough way based on flushing length and the spacing of electrodes as has been done in this paper (Figure 2). At a particular lowering rate, the time of 63% response of the conductivity and temperature sensors can be made equal and this condition represents the optimum in matching of the sensors. Of course, the matching will not be perfect so that even in this optimum case some salinity errors are to be expected in the presence of high gradients.

Frequently, the lowering rate determined by operational considerations is not such that the 63% response of the conductivity and temperature sensors are equal. Since attempting to restore the high frequencies in the data measured by the slower sensor is usually made numerically unstable by the presence of noise and aliased information, the best numerical procedure seems to be to slow the response of the faster sensor in order to produce the best match. (Middleton and Foster (1980), Appendix 1.) In this case, the first step is to compensate for any physical separation of the sensors and separation in sampling times so that both sensors are, in effect, interpolated to the same level and thus begin their responses simultaneously. After this has been accomplished, application of a numerical "time constant" filter to the faster of the two sensors then has the effect of delaying the 63% response by an amount roughly equal to the "time constant". This procedure was accomplished by Middleton and Foster through a series of weights corresponding to the above filter but a more efficient algorithm is given in Otnes and Enochson (1972) as follows:

$$Y_{i+1} = \alpha Y_i + (1-\alpha)x_{i+1}$$

where: $\{Y_k\}$ is the modified time series

$\{x_k\}$ is the measured time series

$$\alpha = e^{-\Delta t/\tau'}$$

τ' is the "time constant" of the filter

Δt is the time between samples

$$\tau' = \tau_s - \tau_f$$

where: τ_s is the time constant of the slower sensor

τ_f is the time constant of the faster sensor

For example, take the case of a 14 cm long conductivity cell whose flushing distance to 63% of its response is 0.55L = 7.7 cm as illustrated in Figure 2. If the lowering rate is 1 m/s, the flushing time or the time constant of the cell is 77 ms. Suppose the time constant of the temperature sensor is 177 ms so that in order to match the two time constants, we need to add 100 ms to the conductivity cell time constant. This can be done,

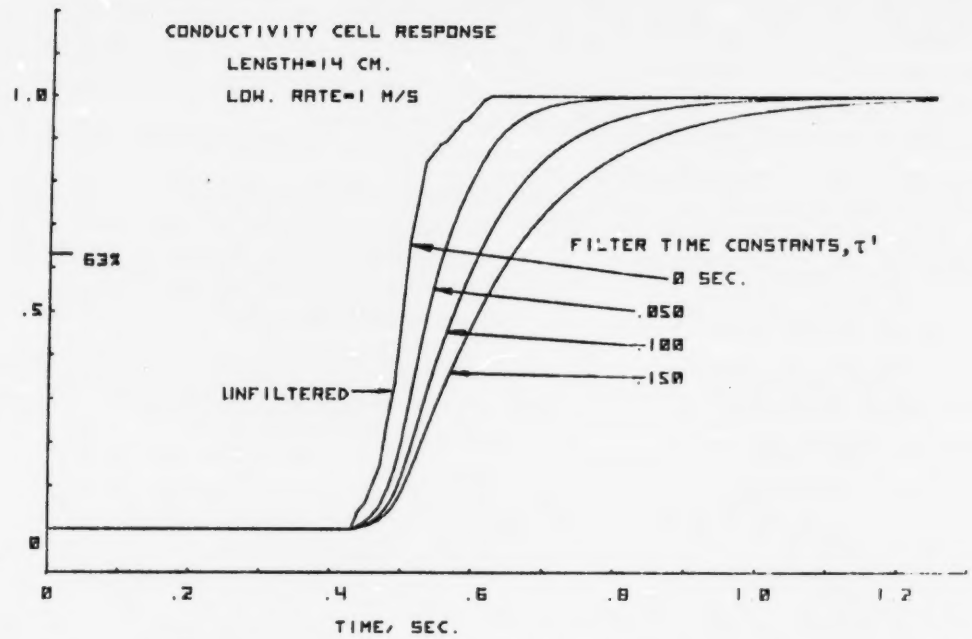

Figure 16. The application of a "time constant" filter to the conductivity cell response given in Figure 2. At the 63% level the delay in response increases by approximately τ' in each case. The curves are more or less independent of the value for Δt used which serves only to define the number of points on each curve.

approximately, by putting $\tau' = 100$ ms. This case and other response curves are illustrated in Figure 16. Suppose also that $\Delta t = 50$ ms so that $\alpha = e^{-50/100} = .607$, then the above equation can be rewritten as

$$Y_{i+1} = .607\, Y_i + .393\, x_{i+1}$$

Note that this procedure is not effective if Δt is very large compared with τ' so that α becomes negligibly small.

Apendix II: Aliasing

Let Δt be the interval at which a signal of frequency f is sampled. With a view to what follows let us represent f as

$$f = \frac{n+p}{2\Delta t}$$

where n is an integer and $0 \leq p < 1$

The signal being sampled is of the form

$$x(t) = \sin(2\pi ft)$$

so that the k^{th} sampled value is

$$\begin{aligned} x(k\Delta t) &= \sin(2\pi fk\Delta t) \\ &= \sin\left[2\pi k\Delta t\left(\frac{n+p}{2\Delta t}\right)\right] \\ &= \sin\{\pi k(n+p)\} \\ &= \sin(\pi kn)\cos(\pi kp) + \cos(\pi kn)\sin(\pi kp) \\ &= \cos(\pi kn)\sin(\pi kp) \\ &= \sin(\pi kp) \qquad \text{(n even)} \\ &= \cos(\pi k)\sin(\pi kp) \qquad \text{(n odd)} \\ &= \sin\{\pi k - \pi kp\} \qquad \text{(n odd)} \end{aligned}$$

Putting $f' = \frac{p}{2\Delta t}$ and $F = \frac{1}{2\Delta t}$ (the maximum value of f') the above expressions become

$$\begin{aligned} x(k\Delta t) &= \sin(2\pi f'k\Delta t) \qquad \text{n even} \\ &= \sin(2\pi(F - f')k\Delta t) \qquad \text{n odd} \end{aligned}$$

When these observations, made at intervals of Δt, are used to describe the continuous function x(t), $k\Delta t$ is replaced by t in the last equations, giving

$$\begin{aligned} x(t) &= \sin(2\pi f't) \qquad \text{n even} \\ &= \sin\{2\pi(F - f')t\} \qquad \text{n odd} \end{aligned}$$

Thus, unless $n = 0$, when $f = f'$, the specified frequency f has been "observed" as a different frequency f' or $(F - f')$. F is called the Nyquist frequency and the phenomenon of frequency shifting due to sampling, aliasing.

The value of f for n = 1, p = 0, is the Nyquist frequency and thus is the lowest frequency for which aliasing occurs. Then $f = 1/(2\Delta t)$ so that sampling occurs twice within each period of f, once each in the positive and negative swings of the sine wave. Physical intuition gives the idea that sampling any more slowly will not allow the sine wave to be resolved and Figure 4 illustrates pictorially the generation of lower frequencies for which an analytic derivation has been given above. If these aliased frequencies are desired, the given frequency, f, should be divided by F to give n and p. If n is even the aliased frequency is pF, if n is odd the aliased frequency is (1 - p)F.

Suppose that a spectrum of frequencies exists sampled at intervals defining a Nyquist frequency F. All the energy of the spectrum will appear in the interval $0 \leq f \leq F$ though in fact the spectrum may contain energies at much higher frequencies. If the true spectral density function is S(f), the apparent density function as measured at that frequency will contain additional contributions from the spectral density at frequencies

(2F + f), (4F + f), (6F + f);... etc. from n even
and (2F - f), (4F - f), (6F - f);... etc. from n odd.

In the ocean the lowering speed of the CTD transfers a spectrum of water structure sizes to frequencies and the above argument applies. However, the time constants of the sensors attenuate the higher frequencies. The longer the time constants in relationship to $2\Delta t$, the period of F, the more will aliased contributions from higher frequencies be attentuated. On the other hand, if the time constants are so long as to virtually eliminate aliasing then significant attenuation will also occur in the interval $0 \leq f \leq F$ where it is undesirable. The optimum combination of time constant and sampling interval depends on the shape of the response curve as well as the tolerable limits of attenuation and aliasing. (Note that, as in previous chapters, "time constant" is used to express the time required for the sensor to reach 63% of the final value in response to a step function irrespective of the curve shape.) The attenuation that any sensor produces for a signal of given frequency may be calculated, and an energy transmission function $\Phi^2(f)$ may be defined by dividing the sensed energy by the incident energy at frequency f. The spectral components resulting from aliasing of frequencies (2F + f), 4F + f)..., (2F - f), (4F - f)..., are then attenuated accordingly so that we may write

$$S_o(f) = \Phi^2(f).S(f) + \Phi^2(2F + f).S(2F + f) + \Phi^2(2F - f).S(2F - f)$$

where $S_o(f)$ is the observed spectrum and only the first two aliased terms have been taken on the assumption that terms from higher frequencies will have been attenuated so as to be negligible. This approach has been used by Sabinin (1967) to produce curves relating aliasing and signal attenuation appropriate for sensors having a simple exponential response. Following Sabinin we have produced Figure 17 which is appropriate for the more complex sensor response shown in Figure 1C. Figure 17A gives the fraction of any power available at frequency (2F - f) that will appear at frequency f in the observed spectrum while Figure 17B does the same for any power at (2F + f). The use of these diagrams is best demonstrated by an example. Consider the sensor and recorder characteristics assumed to produce Figures 6, 7, etc. One entire sample occupied 1 second so that F = ½ Hz. During the period 1/F, the CTD travelling at 1 m/s, moves 2 m so that any oceanic features of wave lengths less than 2 m will suffer aliasing and recorded information will only describe

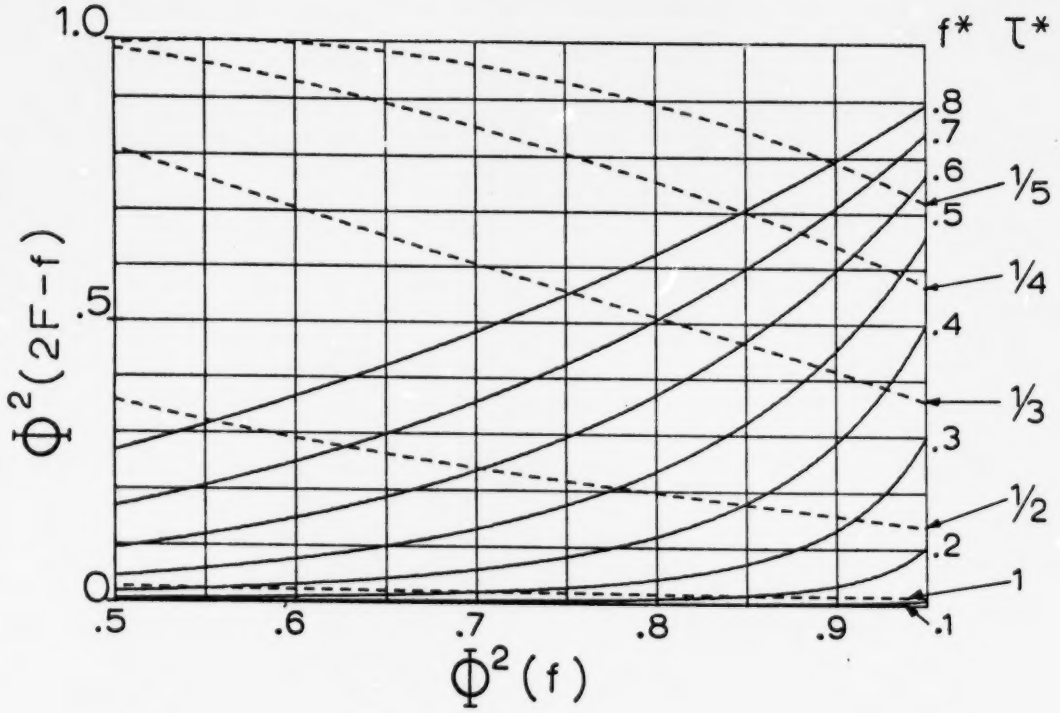

Figure 17A. Nomogram relating frequency of interest, f, sampling interval Δt, time constant τ (for a double exponential sensor response) with signal attenuation Φ^2 (f) and aliasing. F is the Nyquist frequency, equal to 1 ($2\Delta T$) and $\tau^* = \tau/\Delta t$), $f^* = f/F$. Entering with given values at the last two parameters gives signal attenuation at the frequency of interest (abscissa) and the proportion of any power existing at frequency (2F - f) that will be aliased onto the frequency of interest (ordinate).

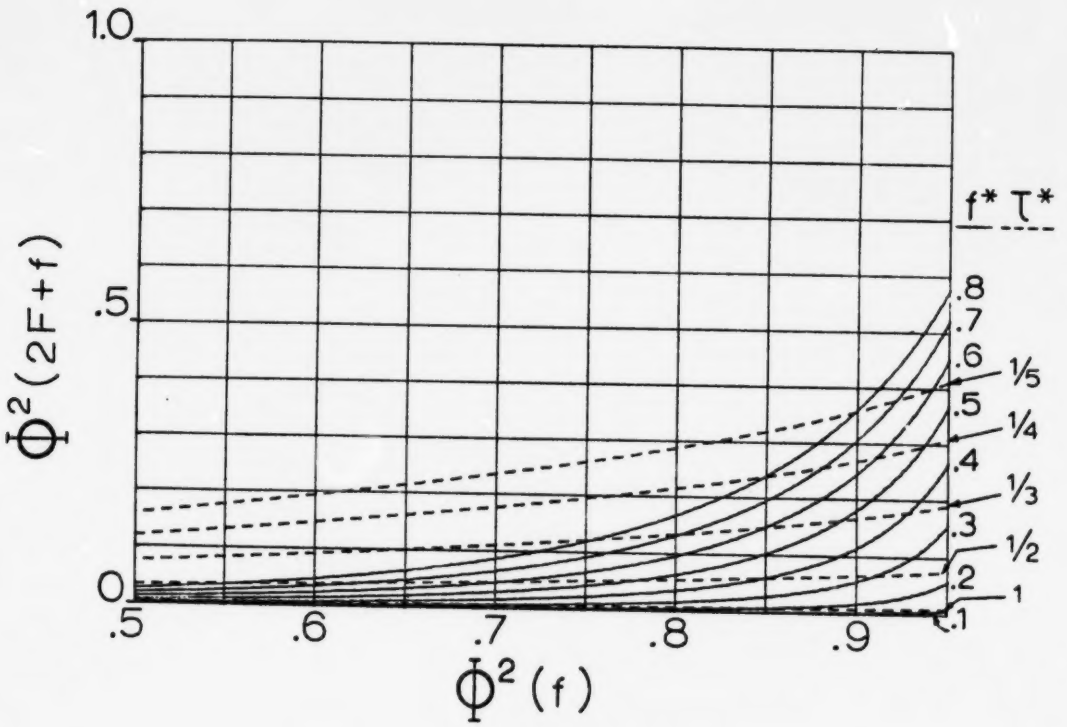

Figure 17B. Nomogram relating frequency of interest, f, sampling interval Δt, time constant τ (for a double exponential sensor response) with signal attenuation Φ^2 (f) and aliasing. F is the Nyquist frequency, equal to $1/(2\Delta T)$ and $\tau^* = \tau/\Delta t$), $f^* = f/F$. Entering with given values of the last two parameters gives signal attenuation at the frequency of interest (abscissa) and the proportion of any power existing at frequency (2F + f) that will be aliased onto the frequency of interest (ordinate).

features longer than 2 m. The temperature "time constant" was 200 ms. This gives values for τ^* of 1/5 to enter Figure 17 where the symbols are defined in the legend. Suppose we are interested in 4 m wave length feature (i.e. f = ¼ Hz) then $f^* = 0.5$. Figure 17 A & B show that about 0.97 of the energy at this wave length will pass the sensor but that about 70% & 43% of any energy existing at lengths of 1 1/3 m (i.e. 2F-f) and 4/5 m (i.e. 2F+f) will become aliased onto the feature of interest. (The lines for $\tau^* = 1/5$, $f^* = 0.5$ must be projected a little beyond the limits of the graphs in this case to get their intersection at $\phi^2(f) = 0.97$.) In surface layers of the ocean, structures with 1 1/3 or 4/5 wavelengths are quite possible and it is likely that some energy will be available for aliasing.

Consider next sampling 25 times per second and a thermometer time constant of 50 ms as is suitable for the Guildline Mk IV machine. At a lowering rate of 1 m/s, samples are taken every 4 cm so that 8 cm oceanic features could be resolved. Significant energy is unlikely to exist at shorter wavelengths but suppose that some does. Let us suppose that interest centres on structures of 50 cm wavelength, corresponding to a frequency of 2 Hz. This gives an F value of 12.5 Hz, $f^* = .16$ and as $\tau^* = 1.2$, it may be seen from Figure 17 that the interesting 2 Hz signal will be passed through the sensor at the 90% level and that a negligible amount of the power available at the aliasing frequencies (23 Hz and 27 Hz) is reflected into the value measured at 2 Hz. This is an excellent design for looking at the ocean in ½ m slices!

Alternatively one may specify the permissible level of transmission $\phi^2(f)$ and aliasing to determine τ^* and f^*.

The situation where the instrument is sampled at intervals equal to or shorter than the time constant is highly desirable. In this case the sample interval does not become a limit to sensing oceanic variations - it is still controlled by the sensor time constants. The example for the Guildline Mark IV given above illustrates this.

Appendix III: Running Mean Filters and Block Averaging

The most frequently used method of filtering data to reduce unwanted high frequency variations is the running mean filter. Although it does not result in a very sharp frequency cut-off, it has the advantage of being computationally efficient and conceptually simple. As the name implies, the N point running mean filter is the average of N consecutive data points.

$$m_j = \sum_{i=-(N-1)/2}^{(N-1)/2} u_{i+j} \Big/ N \qquad \text{(N odd)}$$

$$m_{j+\frac{1}{2}} = \sum_{i=-(N/2-1)}^{N/2} u_{i+j} \Big/ N \qquad \text{(N even)}$$

where m_j is the j^{th} running mean of N points having values u_i

As well as being used as the final smoothing stage in the processing of data, this procedure is used in instruments which are designed to put out averages over the time interval between readings. This sampling scheme, which we will call block-averaging, is equivalent to a running mean filter which, although defined for every time interval Δt, is recorded only every $N\Delta t$. We will consider the effects of operating on this type of data with the time constant compensation scheme recommended in the text. Three cases will be investigated $N\Delta t \sim \tau$; $N\Delta t > \tau$; and $N\Delta t >> \tau$ where τ is the time to a 63% response of the slower sensor.

If $N\Delta t \sim \tau$, the step response is not much changed as is demonstrated in Figure 18. The sensor time response and the averaging procedure are attenuating the same high frequencies and leaving the same low frequencies relatively untouched. Therefore, the compensation scheme is dealing with the same information either before or after averaging and will produce nearly the same correction. Aliasing is effectively eliminated by the filtering effect of the sensor frequency response. Therefore, the time constant compensation scheme recommended in Appendix I may be utilized unchanged. However, in the equation for α, $N\Delta t$ replaces Δt in the index of the exponential function.

If $N\Delta t > \tau$, then data points will be separated by time intervals in excess of the time over which the sensor is capable of responding. Any gradients existing at the time scale of the sensor time constants are not resolved. There is insufficient information to correct the data and yet the averaging effect may not be great enough to eliminate time constant errors at the frequencies of interest. If the time constants are almost matched and sampling occurs so that the sensors occupy the same position when sampled, then the correction will be small in any event. It is advisable to apply the time constant filter before averaging in order to ensure the maximum benefit. However, additional error is unlikely to be introduced by

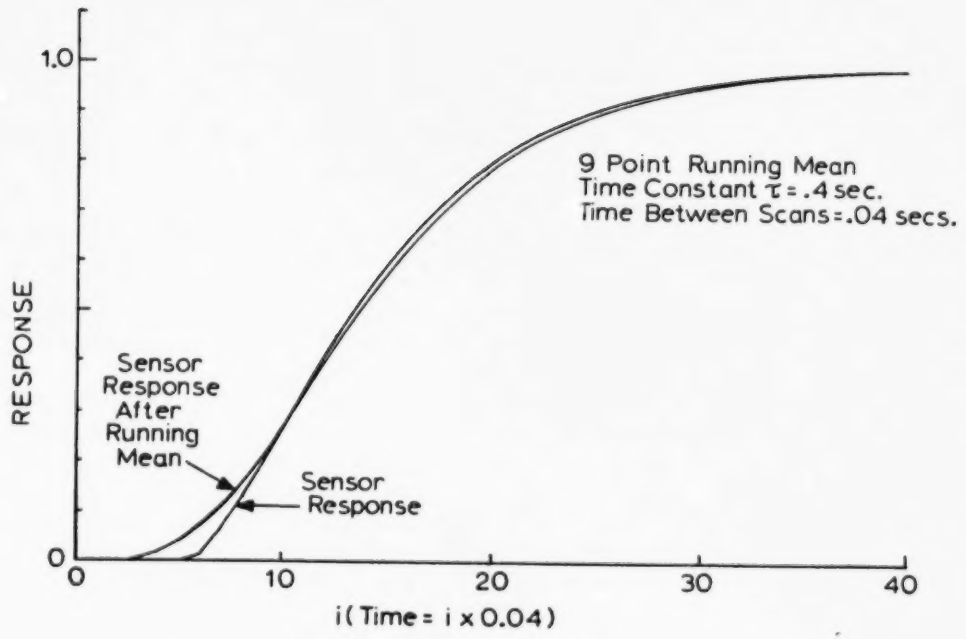

Figure 18. Effect of a 9 point running mean filter on a sensor step response with τ = 0.4 sec. and Δt = 0.04 sec.

reversing these procedures, rather some part of the existing error would not be addressed by the scheme.

If $N\Delta t \gg \tau$, then the effect of the time constant compensation will become vanishingly small through the term $\exp(-N\Delta t/(\tau_1-\tau_2))$ in the equation for α in Appendix I. Therefore, this procedure will have no practical effect on the data. This is due to the attenuation by averaging of frequencies distorted by sensor responses. In addition, the Nyquist frequency, determined by a sampling period of $N\Delta t$, restricts the frequencies detectable to those not much affected by sensor response.

In general, it can be shown by mathematical manipulation that the order of application of a full running mean filter and the time constant compensation scheme recommended here does not matter. Therefore, any errors arising from the block-averaging sampling scheme come about through the loss of the running mean values at data points between the points recorded at times $N\Delta t$.

It may be said that for all practical considerations, the time constant scheme recommended in Appendix I can be used on block-averaged data but that when the block length exceeds about three time constants, i.e. $N\Delta t > 3\tau$, it is unnecessary. However, the results cannot be expected to be as good as results which could be obtained by using all the data available before averaging. If $N\Delta t > 3\tau$, an attempt should be made to either match the time constants or apply a time constant correction before averaging.

References

Acheson, D.T. 1980. Data Editing - Subroutine EDITQ: NOAA Technical Memorandum EOS-CEDDA-6, Center for Experimental Design and Data Analysis, NOAA Washington, D.C. (NTIS accession number PB-257208.)

Fofonoff, N.P., S.P. Hayes, and R.C. Millard Jr. 1974. W.H.O.I./Brown CTD Microprofiler: Methods of Calibration and Data Handling. Woods Hole Oceanographic Institution, WHOI-74-89. Technical Report.

Goulet, J.R. Jr., and B.J. Culverhouse. 1972. STD Thermometer Time Constant. J. Geophys. Res., 77: 4588-4589.

Gregg, M.C. and T.B. Meagher. 1980. The Dynamic Response of Glass Rod Thermistors. J. Geophys. Res., 85: No. C5.

Middleton, J.H. and I.D. Foster. 1980. Fine Structure in a halocline. J. Geophys. Res., 85: No. C2.

Millard, R., J. Toole, and M. Schwartz. A Fast Responding Temperature Measurement System for CTD Applications. Ocean. Eng., 7: 413-427.

Lewis, E.L. and R.B. Sudar. 1972. Measurement of Conductivity and Temperature in the Sea for Salinity Determination. J. Geophys. Res., 77: 6611-6617.

Paige, M.A. 1978. Response Characteristics of the NBIS INC. Mark III CTD to Step Changes in Temeprature and Conductivity. Naval Oceanographic Office, Bay St. Louis, Mississippi. Internal Report.

Roden, G.I. and J.D. Irish. 1975. Electronic Digitization and Sensor Response Effects on Salinity Computation from CTD Field Measurements. J. Phys. Ocean. Vol. 5.

Sabinin, K.D. Selection of the Relation Between the Periodicity of Measurement and Instrument Inertia in Sampling. Izv. Akad. Nauk., S.S.S.R., Atmospheric and Oceanic Physics, 3, 5; 973-980.

Saunders, P.M. and N.P. Fofonoff. 1976. Conversion of Pressure to Depth in the Ocean. Deep-Sea Research, 23: 109-111.

Walker, E.R. 1978. Laboratory Determination of the Responses of Thermometer and Conductivity Cell of the Guildline 8101A, I.O.S. Note 7. Institute of Ocean Sciences, Patricia Bay, Sidney, B.C.